UCLA
UCLA Electronic Theses and Dissertations

Title
Digital Loop-Mediated Isothermal DNA Amplification

Permalink
https://escholarship.org/uc/item/6fk060c8

Author
Kong, Janay Elise

Publication Date
2017

Peer reviewed|Thesis/dissertation

eScholarship.org Powered by the California Digital Library
University of California

UNIVERSITY OF CALIFORNIA

Los Angeles

Digital Loop-Mediated Isothermal DNA Amplification

A dissertation submitted in partial satisfaction of the

requirements for the degree Doctor of Philosophy

in Bioengineering

by

Janay Elise Kong

2017

© Copyright by

Janay Elise Kong

2017

ABSTRACT OF THE DISSERTATION

Digital Loop-Mediated Isothermal DNA Amplification

by

Janay Elise Kong

Doctor of Philosophy in Bioengineering

University of California, Los Angeles 2017

Professor Dino Di Carlo, Chair

Nucleic acid amplification has applications in diagnostics, sequencing, genetic fingerprinting, among others. Currently nucleic acid amplification is treated as the "gold standard" method for several diagnostics; however, because of the multi-step protocols and the large equipment, these assays are lengthy and require laboratory settings. Digital nucleic acid amplifications assays developed have greatly improved several aspects of nucleic acid amplification by creating a more robust and sensitive assay. This is due to the reduction in background noise and the ability to effectively concentrate target analytes in nano- or picoliter volumes by compartmentalization of these samples. We were able to demonstrate a 69-fold fluorescence change in an isothermal nucleic acid amplification assay, with a >60% increase in fluorescence stability with elevated temperatures over the time course of the reaction, with the use

of a unique dye combination of EvaGreen and hydroxynapthol blue (HNB). Due to the improvements in signal, we were able to demonstrate comparable results using a mobile phone based fluorescence plate reader as with that of a benchtop reader. The unique dye combination was then applied to a digital system, demonstrating signal improvements that are crucial to developing a robust assay, giving a higher efficiency (percentage of "on" wells closer to the theoretical value) and a larger difference in fluorescence intensities for "on" versus "off" wells. Lastly, we examined the mechanism of the dye combination to best determine additional ways of improving the signal generation. By sequestering EvaGreen, HNB allows amplification to proceed without interference. Additionally, a Förster resonance energy transfer (FRET) interaction between the dye molecules, when DNA is absent from the solution, acts to lower the background fluorescence such that a greater fluorescence fold change occurs with DNA amplification. The EvaGreen and HNB have a highly-tuned binding affinity such that prior to DNA amplification, they have FRET interactions, and afterwards in the presence of large amounts of DNA, EvaGreen binding to DNA becomes more favorable. All of these developed technologies and methods work in conjunction to improve upon currently developed techniques for nucleic acid amplification in point of care settings.

The dissertation of Janay Elise Kong is approved.

Aydogan Ozcan

Paul S. Weiss

Ren Sun

Dino Di Carlo, Committee Chair

University of California, Los Angeles

2017

Dedication

For my mom and dad who pushed me to strive for more, my family who continually supports me, and all of the younger generations who I can hope to inspire.

Contents

Chapter 1: Sensing Nucleic Acids and Proteins Using Microfluidic Digital Assays 1

1.1 Microfluidic Digital Assays 1

1.2 Sample Fractionation..... 3

1.2.1 Microwells 4

1.2.2 Micro-emulsions 4

1.3 Microfluidic Digital Assays 6

1.3.1 Digital Nucleic Acid Amplification 7

1.3.2 Isothermal Digital Nucleic Acid Tests for Distributed Testing..... 9

1.3.3 Digital Immunoassays 10

1.4 Future Directions with Digital Assays 12

Chapter 2: Sensitive and Stable Nucleic Acid Amplification with Cell-phone Based Readout 14

2.1 Introduction 15

2.2 Results and Discussions 18

2.2.1 Enhancing Intercalating Dye Performance with Hydroxynapthol Blue 18

2.2.2 Mobile Phone Based Fluorescent Plate Reader Performance 24

2.3 Conclusions 29

2.3 Materials and Methods 32

2.3.1 LAMP Assay 32

2.3.2 Temperature Studies with EvaGreen and HNB 34
2.3.3 Cell-phone based portable fluorescent microplate reader 34
2.3.3 Characterization of the Limit of Detection (LOD) 35
2.3.4 Intensity Normalization of Wells 36
Chapter 3: Digital Loop-mediated Isothermal DNA Amplification (LAMP) 37
3.1 Introduction 38
3.2 Results and Discussion 39
3.3 Conclusions 46
3.4 Materials and Methods 47
Chapter 4: Digital Loop-mediated Isothermal DNA Amplification (LAMP) 49
4.1 Introduction 49
4.2 Results and Discussion 50
4.3 Conclusions 53
4.4 Materials and Methods 53
4.4.1 Compression Device Fabrication 53
4.4.2 Digital LAMP 54
4.4.3 Image Processing and Normalization 54
Chapter 5: Conclusions 56
Appendix A 58
References 64

Acknowledgments

Chapter 1 contains the publication: Kong JE. and Di Carlo, D. (2016) “Sensing Nucleic Acids and Proteins Using Microfluidic Digital Assays”. ACS Sensors (in progress) JEK wrote the manuscript. JEK, DD revised the manuscript.

Chapter 2 is adapted from the publication: Kong JE, Wei Q, Tseng D, Zhang J, Pan E, Lewinski M, Garner OB, Ozcan A. Di Carlo D. "Highly stable and sensitive nucleic acid amplification and cell-phone based readout." ACS Nano. 2017 JEK, QW, DT, JZ, and EP performed experiments and analyzed data. JEK, QW, and DT prepared the manuscript. ML, OBG, AO, and DD provided guidance throughout the work and manuscript.

The author and work was supported by funding from the National Science Foundation Emerging Frontiers in Research and Innovation Award (Grant #1332275).

VITA / BIOGRAPHICAL SKETCH

PREVIOUS EDUCATION

M.S. Biomedical Engineering (2012), University of California, Los Angeles

B.S. Bioengineering (2009), Cornell University, Ithaca, NY

RESEARCH APPOINTMENTS

03/12 – 3/17 Graduate Student Researcher, University of California, Los Angeles

Professor Dino Di Carlo, Microfluidic Biotechnology

WORK EXPERIENCE

01/12 – 03/13 Teaching Assistant, University of California, Los Angeles

Bioengineering 167L (03/12–06/12), Bioengineering 177A & B (9/12-3/13)

PUBLICATIONS

1. Kong JE, Di Carlo D "Sensing nucleic acids and proteins using microfluidic digital assays" (in progress)
2. Kong JE, Wei Q, Tseng D, et. al. (2017). "Highly stable and sensitive nucleic acid amplification and cell-phone based readout." ACS Nano.
3. Tseng P, Lin J, Owsley K, Kong JE, et al. (2015). " Flexible and Stretchable Micromagnet Arrays for Tunable Biointerfacing." Advanced Materials. 27(6):1083-1089.
4. Kong JE, Koh J, Lin J, Di Carlo D. (2015). "Research highlights: translating chips." Lab on a Chip. 15 (9):1984-1988.
5. Kim D, Wei Q, Kong JE, Di Carlo D. (2015). “Research highlights: digital assays on chip.” Lab on a Chip. 15 (1):17-22.

6. Kong JE, Kahkeshani S, Pushkarsky I, Di Carlo D. (2014). “Research highlights: micro-engineered therapies.” Lab on a Chip. 14(24):4585-4589.
7. Munoz HE, Che J, Kong JE, Di Carlo D. (2014). “Advances in the production and handling of encoded microparticles.” Lab on a Chip 14(14):2212-2216.

PRESENTATIONS

1. Kong JE, Margolis M, Di Carlo D. “Intercalating dye sequestration for order of magnitude improvement in signal applied to digital nucleic acid amplification tests.” Poster presentation at MicroTAS. 2016 October 9-13; Dublin, Ireland.
2. Kong JE, Kim D, Di Carlo D. “Exponentially amplified isothermal immunoassay with size-based oligonucleotide background reduction.” Poster presentation at MicroTAS. 2015 October 25-29; Gyeongju, South Korea.
3. Kong JE, Kim D, Di Carlo D. “Exponentially amplified isothermal immunoassay with size-based oligonucleotide background reduction.” Oral presentation at Biomedical Engineering Society Annual Meeting. 2015 October 7-10; Tampa, FL.
4. Kong JE, Murray C, Di Carlo D. "Magnetic manipulation with customizable bioactive superparamagnetic nanoparticles." Oral presentation at Biomedical Engineering Society Annual Meeting. 2013 September 25-28; Seattle, WA.

HONORS AND AWARDS

Graduate Division Fellowship (Spring 2012)

Chapter 1: Sensing Nucleic Acids and Proteins Using Microfluidic Digital Assays

Digital assays have been used to detect and quantify nucleic acids and proteins with greater reproducibility and sensitivity than conventional assays. Conventional assays have limitations when it comes to detecting and quantitating low concentrations of target molecules. By splitting a sample into distinct small volumes, single target molecules and reaction products can be effectively concentrated, facilitating detection in that small volume. Digital assays with their binary outputs have the potential for single molecule level resolution, making them ideal for identification of rare variants, while also being robust to assay conditions and reduced calibration procedures. While digital assays are able to improve sensitivity and repeatability, the assay complexity and equipment needs currently limit their use to laboratory-based settings.

1.1 Microfluidic Digital Assays

Microfluidics technology allows for the control and manipulation of very small amounts of fluids – several orders of magnitude smaller in volume than can be reasonably manipulated using benchtop fluid pipetting[1]. Using this technology large volumes containing entities (e.g. molecules or cells) to be detected can be fractionated into thousands of nano-, or even picoliter volumes that contain either one or zero of a particular entity of interest. By creating barriers to reaction between volumes (fractionation), using microemulsions or microwell technology, each of these separate volumes can be assayed individually in a high throughput manner[2]. Such "digital" assay versions of conventional molecular biology assays, including digital polymerase chain reaction (PCR) and digital enzyme-linked immunosorbent assay (ELISA), can provide unique capabilities. By splitting the sample into small enough volumes, each well or droplet will in most

cases have either a single target molecule present or none, such that following a sensing reaction, a binary output signal of "on" or "off" can be determined. By simply counting the fraction of "on" compartments, one can more directly see and quantify the amount of target analyte in solution, proving advantageous to conventional methods that require the generation of a standard curve and careful assay calibration (**figure 1.1**). However, there are also tradeoffs with digital assays. For example, because digital assays depend on an assumption of at most one target analyte per well, the dynamic range is limited by both the minimum volume of each compartment and the total assay volume.

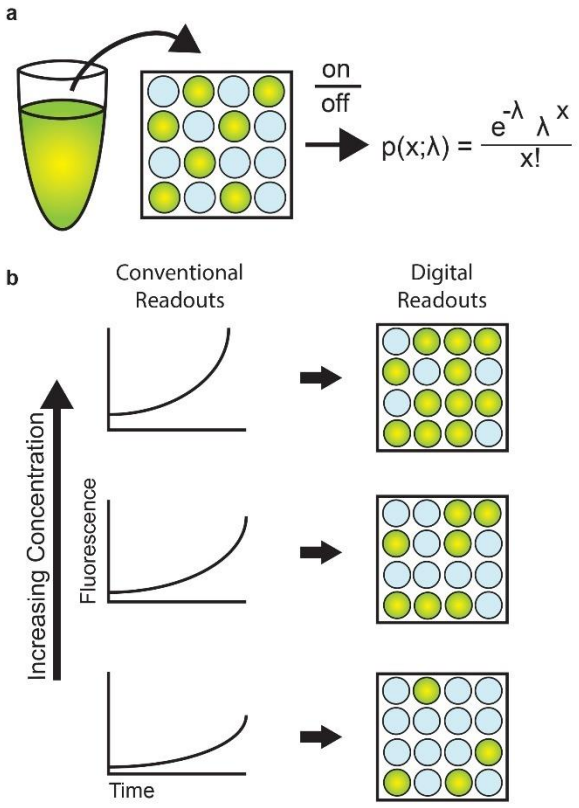

Figure 1.1. *a. In a digital assay, large volumes are split into small compartments to produce a binary "on" or "off" signal if solutions are sufficiently dilute to allow Poisson occupancy statistics. This allows determination of the initial target concentration. b. Comparison between analog and digital readouts.*

1.2 Sample Fractionation

One of the key steps in a digital assay is compartmentalizing the volume into smaller fractions. Sample fractionation is typically achieved using a microfluidic device, either in wells[3] or in droplets[4] (**figure 1.2**). Both approaches allow rapid fractionation of a sample to relatively uniform nanoliter or sub-nanoliter scale volumes, but have unique trade-offs.

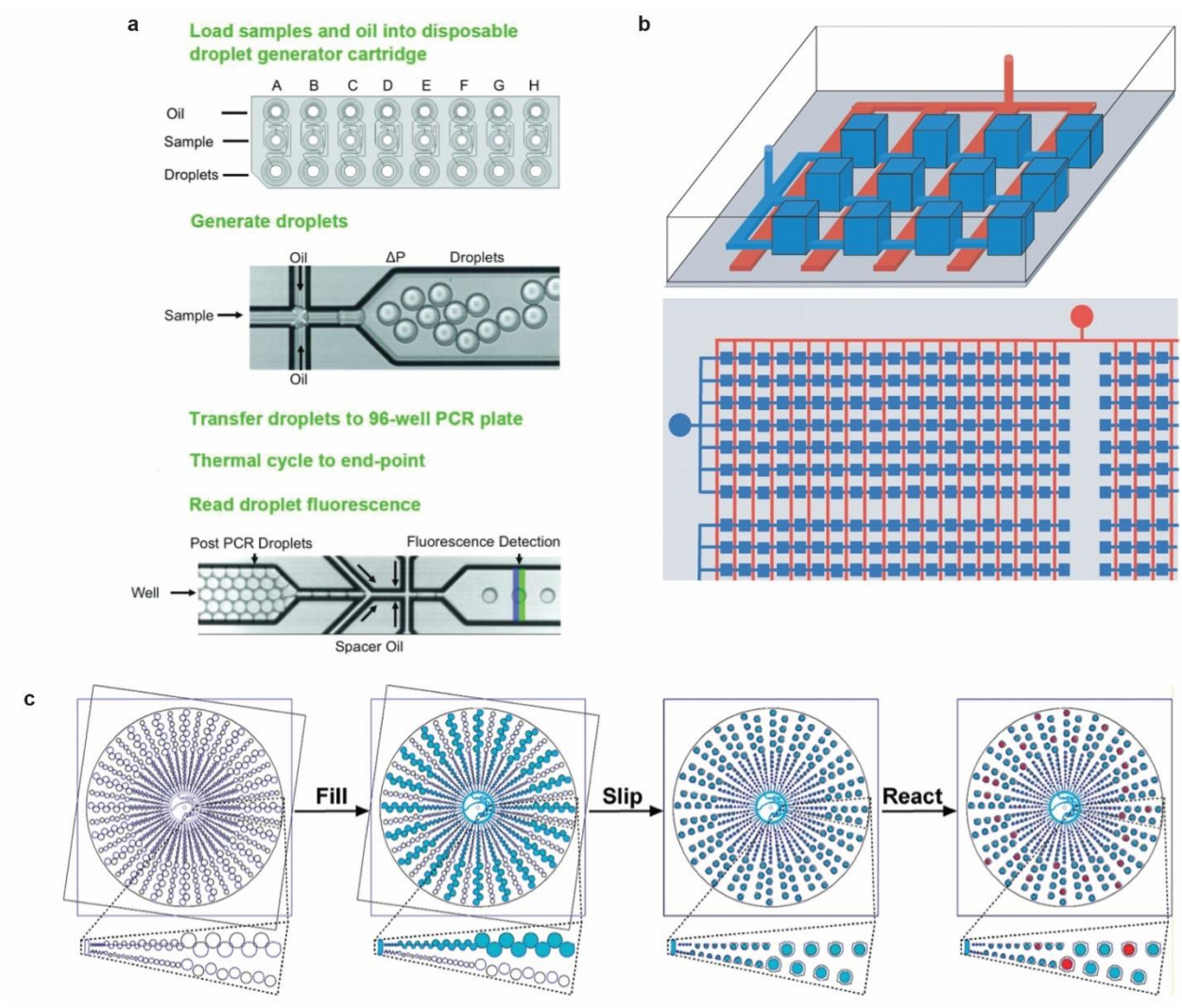

Figure 1.2. *Different ways a sample can be fractionated, using microfluidics a. with a droplet generator. Adapted with permission from Hindson et al.*[5]*. Copyright 2011 American Chemical Society. b. with a system of wells and valves for sealing. From Ottesen et al.*[6]*. Adapted with permission from AAAS. c. with a SlipChip. Adapted with permission from Shen et al.*[7]*. Copyright 2011 American Chemical Society.*

1.2.1 Microwells

Digital assays in wells typically allow for more flexibility in sample preparation, for example, with beads that can be functionalized to capture target molecules and then incubated and washed with multi-step additions of new solutions. Additionally, viscosity, surface tension, and flow rates do not affect the uniformity of sample volumes which can be precisely controlled. However, one limitation inherent to wells as opposed to droplets, are the effects of surface fouling. Given the high-surface area, reaction components such as proteins, enzymes, of nucleic acids can adsorb to surfaces, leading to variation in reaction kinetics compared to a bulk reaction. Although steps can be taken to block surfaces and limit the effects of nonspecific binding, these add more assay complexity, and result in a surface environment that still is not similar to the bulk solution, often leading to reduced performance. One such technique to generate wells that also allows for multi-step additions of reagents is called the SlipChip[8,9]. Using this device allows for uniform volumes of fluid to fill compartments, and then a subsequent 'slip' step shifts the wells to have physical continuity with other wells such that they combine with other contained solutions on this different area of the chip.

1.2.2 Micro-emulsions

Droplet microfluidics and drop-based assays offer unique advantages. The generation of thousands of droplets per second[10] enables the development of high throughput assays that allow for the flexibility in sample volumes tested without redesigning the device. When analyzing larger volumes, flowing droplets past an optical excitation and sensing point can allow for sensing each droplet individually using a fluorescent, colorimetric, or other readout approach. Because one can continually produce more droplets with the same device, droplet microfluidics can provide increased scalability without the need to change the device geometry or area of well arrays. As a

result of Poisson statistics, larger droplets shift the dynamic range (the concentration range for which digital readout is possible) towards a lower limit and conversely smaller droplets shift the dynamic range upward for the same overall tested volume. The largest and smallest volume of "micro-reactors" in an assay determines the assay's dynamic range, and while it is possible to simply dilute out the sample in order to quantitate larger analyte concentrations, running an assay multiple times in order to accommodate differing concentrations is not ideal. Creating a mixture of both large droplets to expand the overall tested volume and small droplets to allow sampling a higher concentration range within the same device can allow a significant extension of the dynamic range. As droplet size changes with flow rate with many flow-focusing or T-junction droplet generators, a single device can be utilized to make a range in droplet sizes (**figure 1.3**). Droplets can also be manipulated to allow for merging, or exchange of fluid, such that multi-step reactions can occur in each droplet[11–13]. Multi-step reactions, requiring exchange of fluids, or sequential addition of reagents, that are possible in both droplets and wells enable greater flexibility in assay development. Each reaction step can operate under different reaction conditions, and reagents can be added only when needed to limit interference, potentially leading to an overall increase in assay efficiency. Standard droplet generation systems generally require precise control over fluid flow, which leads to larger and more bulky equipment, limiting use to laboratory settings. This makes this equipment harder to translate for use in the field or point-of-care diagnostics.

In summary, both compartmentalizing in wells or droplets can enable digital assays, but larger volumes are difficult to analyze. Droplets have the advantage of flexibility of droplet size and number, enabling a larger dynamic range within a single device. Fabricated wells have the advantage of ease of imaging because of the precise well locations set up in a known pattern, while wells typically create more monodisperse volumes because of the microfabrication techniques employed are highly uniform. One of the current limitations of digital assays is the ability to only

assay a small volume, usually smaller than traditional assays because of the large number of micro-compartments that need to be imaged per unit volume. While continuous flow droplet generation systems provide the ability to create more droplets, this process takes time for both droplet generation and imaging and further processing afterwards.

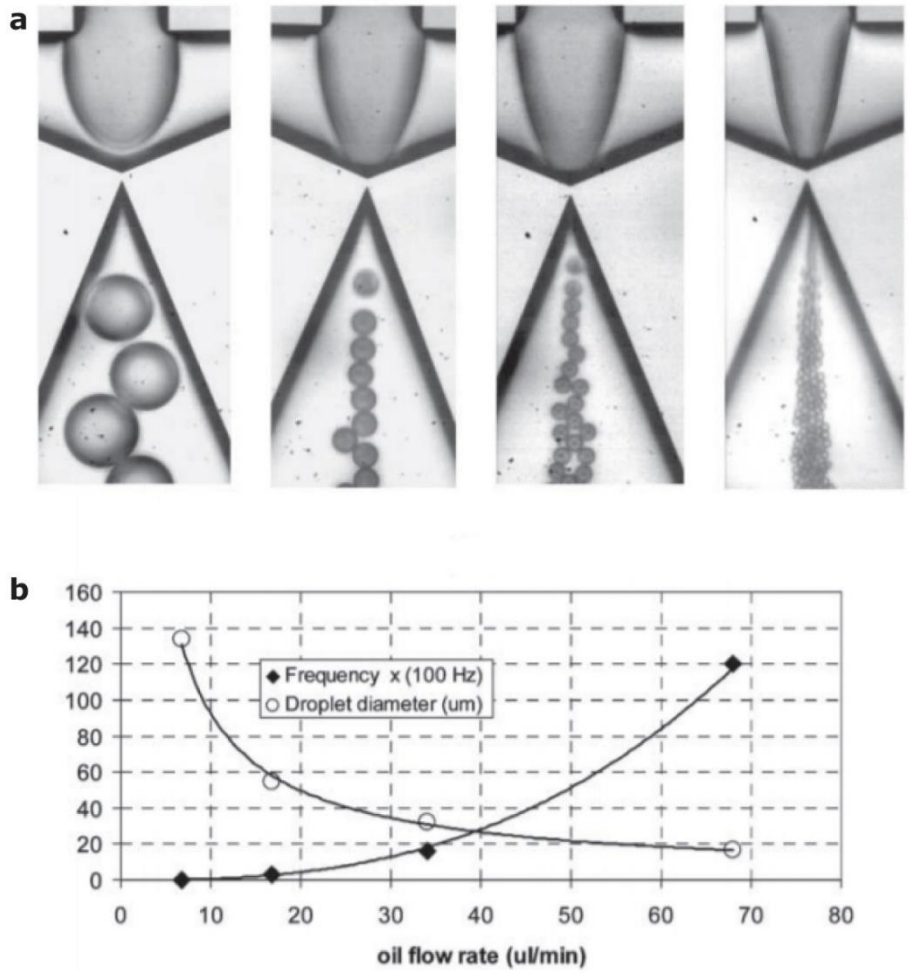

Figure 1.3. *a. Water in oil droplet formation at a constant water flow rate, and increasing oil flow rates (left to right) b. Droplet diameter and generation frequency from the above images. Adapted from Yobas et al.*[14] *with permission from The Royal Society of Chemistry.*

1.3 Microfluidic Digital Assays

The field of digital assays has primarily been split into two subgroups: digital nucleic acid amplification tests and digital immunoassays or ELISAs. These two assays are well-suited to

digital approaches because the binary assay outputs make these assays less dependent on enzymatic activity of the polymerase or other signal-generating enzymes, producing more repeatable results with a single measurement. By treating each compartment as an individual micro-reactor, target analytes can be measured down to the single molecule level. In a digital assay, the limit of detection (LoD) often depends on the amount of sample analyzed, assuming that false positive compartments with signal are not prevalent. Larger compartment volumes contain more sample and therefore have an increased probability of containing the target molecule, but also potentially contaminating molecules that reduce the uniqueness of the signal. Digital assays improve the LoD by limiting the noise in each volume and sequestering contaminating compounds to a small subset of volumes instead of the entire volume, through physical barriers. For example, if there is contamination in a sample, a conventional assay will give a positive signal, whereas in a digital assay, only a small number of wells out of thousands will have a positive signal.

1.3.1 Digital Nucleic Acid Amplification

Several digital nucleic acid amplification methods have been developed and even commercialized[15]. The first demonstration by Vogelstein et al. examined the use of limiting dilutions in order to improve assay sensitivity and postulated that the limit of detection was only limited by the number and volume of compartments analyzed[16]. This seminal work was completed in both 96- and 384-well plates by pipetting, including a secondary probe addition, which made performing these assays very tedious. In a microfluidic format, nucleic acid amplification has been accomplished in both droplets and wells using the gold standard PCR, as well as a number of isothermal nucleic acid amplification techniques. Commercially available digital PCR technologies have been developed by Fluidigm, RainDance, Stilla and BioRad (**table 1.1**) using both wells and droplet-based approaches[15], and new technologies continue to come to market.

Digital PCR often has followed the protocols of standard qPCR, but has some unique capabilities. Like the standard for qPCR methods, several of these technologies require the use of a reference dye, e.g. ROX, in order to account for differences in droplet volumes or a baseline shift in fluorescence. A number of these technologies also require the use of customized Taqman probes for each target DNA sequence. Digital PCR has been found to be more robust than standard qPCR when testing the reaction against possible inhibitors[17]. However, both with digital PCR and with isothermal assays such as loop-mediated isothermal DNA amplification (LAMP), the assay susceptibility to inhibitors varied with the inhibitor used. Specific to nucleic acid amplification assays, the digital systems do not take into account amplification bias for different target sequences.

Table 1.1. *Commercial digital PCR technologies. Reprinted by permission from Macmillan Publishers Ltd: Nature Methods. Baker, M.*[15]*, copyright 2012.*

Vendor	Instruments and list price	Consumables and list price	Number and volume of partitions	Volumes required	qPCR capacity	Multiplexing
Fluidigm Corporation	BioMark HD: $200,000–$250,000	12 arrays per chip[a] (765 wells per array): $400 per chip (works in both EP1 and BioMark)	12-inlet chip: 9,180 partitions, 6 nl per partition	12-inlet chip: 8 μl of mix, ~4 μl of sample; 57% analyzed[b]	Yes	Can use up to 5 colors to detect 5 targets (assumes 5th color is ultraviolet)
	EP1: $100,000–$150,000	48 arrays per chip[a] (770 wells per array): $800 per chip (works in both EP1 and BioMark)	48-inlet chip: 36,960 partitions, 0.85 nl per partition	48-inlet chip: 4 μl of mix, ~2 μl of sample[b]	No	Can use up to 5 colors to detect 5 targets
Life Technologies	OpenArray RealTime PCR System and QuantStudio 12K Flex instrument: $140,000 and $90,000–$190,000, respectively	OpenArray plates[a] (64 holes per subarray): $150 per plate	Varies; 3,072 partitions per plate, 48 subarrays per plate, 33 nl per partition (machines run 3–4 plates at once)	100 μl of sample per plate (across 48 arrays)	Yes	Uses 2 colors of probes to detect 2 targets
Bio-Rad Laboratories	QX100 ddPCR System (machines to generate and read droplets): $89,000	8 samples per chip (14,000–16,000 droplets per sample): $3 per sample	Up to 96 samples per run (assumes manual pipetting into PCR plate); 1,344,000 partitions per run (assuming separate thermocycler runs 12 chips at once), 1 nl per partition	Up to 9 μl per sample (20,000 droplets made); an average of 70% read	No	Uses 2 colors to detect 2 targets
RainDance[c]	RainDrop Digital PCR (machines to generate, collect and read droplets): $100,000	8 samples per chip (up to 10,000,000 droplets per sample): $10–$30 per sample	8 samples per run; up to 80,000,000 partitions per run, 5 pl per partition	5–50 μl per sample	No	Uses 2 colors, but can use varying concentrations of probes to detect up to 10 targets

[a]Arrays can hold separate samples, or the same sample can be spread over multiple arrays. [b]For rare allele analysis, protocols are available to eliminate the dead volume. [c]Plans full commercial launch later this year.

Digital PCR can enhance performance in the presence of contaminants or non-target sequences. PCR is very prone to contamination, and often after several cycles, signal amplification occurs, even without the presence of the target DNA sequence. As discussed, physically separating volumes from one another limits contamination to a subset of the volumes in digital PCR and therefore can reduce effects of inhibitors or other contaminants. Interrogating thousands of individual compartments enables a highly sensitive assay that coincides with a low LoD, owing to the large number of compartments and sample volume analyzed. Digital nucleic acid amplification, as with other digital assays operate based on the idea that an absolute quantification of target analyte can be obtained by counting each individually amplified compartment. This is based on the assumption that each target analyte will not only trigger an amplification reaction, but also generate a signal detectable above background. While it has been demonstrated that digitization can improve reproducibility of PCR[18,19], typically these assays underestimate target analyte[8], making a calibration curve necessary for true quantification, despite claims otherwise. Target analyte underestimation can result from a variety of cases that limit amplification, such as target nucleic acid molecules nonspecifically binding to the walls of wells or interfaces of drops, damage to target molecules, decreased enzymatic activity due to surface interactions, etc. Reactions near surfaces or interfaces is an active area of research and further investigation will be necessary to uncover all of the causes of the surface-based variation in performance with these assays.

1.3.2 Isothermal Digital Nucleic Acid Tests for Distributed Testing

Other digital nucleic acid amplification tests, such as loop-mediated isothermal amplification may address challenges in achieving distributed digital nucleic acid sensors. Because of the bulky instrumentation requirements for pressure control and thermocycling, most digital PCR assays

have been limited to a laboratory based setting. Emerging isothermal amplification technologies such as LAMP[20], strand displacement assays (SDA)[21], rolling circle amplification (RCA)[22], and nicking enzyme amplification reaction (NEAR)[23], are flexible and insensitive to slight variations in temperature. Because of this, these assays may be able to be performed more easily, faster, or with increased sensitivity and specificity. Additionally, due to the thermocycling of PCR, commercial instruments require separate devices or instrumentation for each step of the process, from sample fractionation and thermocycling to imaging and readout. Like other digital assays, digital isothermal amplification, such as digital LAMP can also be performed in droplets[24], in microwells[17], and also can include multi-step additions to the assay[8]. Like digital PCR, digital LAMP has been shown to provide reproducible results and an improved quantitative range as opposed to the analog counterpart[17]. Moreover, by implementing a continuous flow digital assay, the sample volume is dynamic and can be altered depending on the needs of the assay[24]. However, these assays tend to struggle with the development of a large signal to noise ratio, leading to a relatively high limit of detection. Additionally, this particular assay requires the use of a reference dye, only adding to the imaging complexity and post-processing. In addition to a more complex device fabrication, this digital LAMP assay also requires a confocal imaging platform.

Both digital PCR and digital LAMP have been shown to provide more repeatable results than their analog counterparts, without the need for generating a standard curve. However, there are a number of limitations and improvements that can be made to facilitate a more efficient, sensitive, and specific assay that is also easy to use.

1.3.3 Digital Immunoassays

In addition to nucleic acid amplification and detection, immunoassays such as ELISA have been successfully demonstrated in digital microwell formats[3,25] (**figure 1.4**). The ability to detect

target analytes down to a single molecule level promises to be revolutionary for a number of different diagnostics. Like the digital nucleic acid amplification techniques, digital implementations of ELISA can improve sensitivity and detection of low analyte concentrations. Although highly sensitive, there are a number of improvements that can be made to facilitate the assay's ease of use and further push the boundaries for lower limits of detection, shorter processing times, improved sensitivity, and integration with standard laboratory materials. Assay processing time for one reported digital ELISA approach[3] is approximately 6 hours, with several wash and incubation steps. This compares to 4-5 hours for a standard ELISA, however, the LOD falls from 10^{-15} to 10^{-16} M with a standard assay to 10^{-15} to 10^{-19} M with the digital assay. Both in an ideal sample as well as in clinically relevant samples, the long assay processing time may be worth the wait.

Like analog assays, digital assays can also be multiplexed, with a multiplexed digital ELISA developed recently to detect four different analytes at a low to sub pg/mL level[26]. By encoding different antibody labeled beads with varying fluorophores, Rissin et al. were able to transform a single analyte sensor into a multiplexed assay. The ability to detect multiple target analytes in a single assay is extremely favorable, decreasing the number of assays needed to be run for a single diagnosis and allowing for calibration between analytes. The trade-off is that by filling wells with one of many possible targeting beads, the number of individual reactions for each target is reduced given the same overall tested volume, effectively decreasing the assay's overall sensitivity, resulting in a higher limit of detection for each target analyte. One can improve upon this, by merely adding more wells, and processing the sample at a larger scale[27]. By utilizing over a million femtoliter wells, a LoD of 10 zM was achieved[27]. Additionally, the large number of reaction chambers acts to improve the assay's dynamic range, an issue that limits all digital assays. With an assay this large, imaging and processing the large field of view can then become a

technical issue from the optical system design and computational requirements. Digital ELISAs and emerging technologies hold significant promise for more robust, repeatable, sensitive, and specific assay that can detect target analytes down to the single molecule level, but the assay accessibility and ease of use have much that can be improved upon in the coming years.

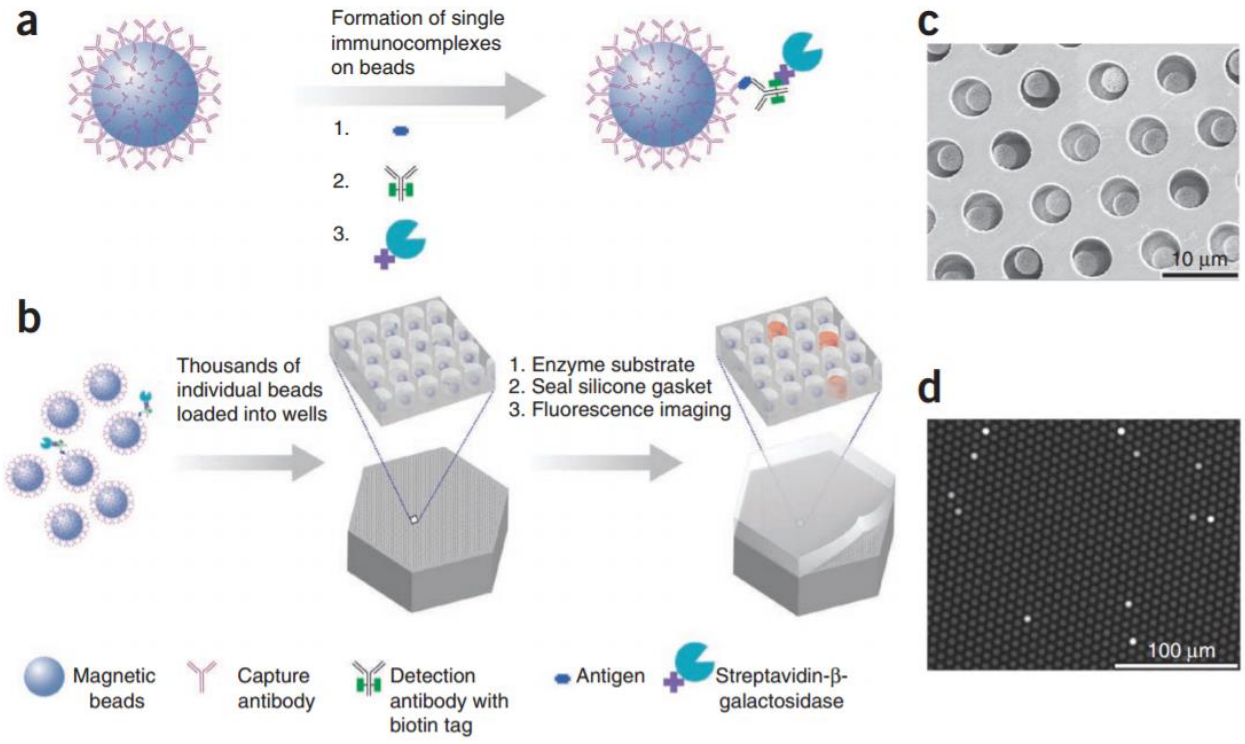

Figure 1.4. *Digital ELISA using beads and femtoliter wells. a. Target analytes are captured to form immunocomplexes on beads. b. Beads are loaded into wells and then an enzymatic substrate is added before the wells are sealed and fluorescently imaged. c. Scanning electron micrograph of beads loaded into the device. d. Fluorescence micrograph of a section of the device, depicting a small fraction of "on" wells. Reprinted by permission from Macmillan Publishers Ltd: Nature Biotechnology. Rissin, D. et al.* [3]*, copyright 2010.*

1.4 Future Directions with Digital Assays

One method that has been proposed to expand the dynamic range of these assays is to combine fractionation with an analog readout for higher concentration ranges that would lead to single digit numbers of molecules per well[28]. This approach assumes that the response is uniform for each molecule and can be linearly superposed. For concentrations with 70% or lower active

beads, a digital readout is measured and for concentrations above, an analog fluorescence measurement is performed. This adjustment in the way the signal is measured and subsequently analyzed can improve the dynamic range by almost two logs of concentration without the need to adjust the assay conditions. The ability to measure the fluorescent signal accurately using analog methods still depends primarily on the imaging system and also on the ability of the assay to generate a high enough differential signal such that a single amplification event can be distinguished from multiple.

Digital assays have provided a robust and sensitive platform for a variety of assays from nucleic acid amplification tests to immunoassays. The instrumentation and devices used are also translatable to other assays such as single-cell analyses[29–31]. While the current assays hold a lot of promise for the detection of target analytes, these techniques are primarily limited to laboratory based settings. Isothermal DNA amplification techniques have made strides in the translation of digital nucleic acid amplification assays to the field; however, further innovations are necessary to transfer the entire process to field-portable settings. Low signal generation necessitates more expensive and sensitive optics, preventing the adoption of these techniques into point-of-care sensors. Compartmentalization of volumes, either in droplets or wells, typically requires the use of bulky equipment, such as syringe pumps to generate monodisperse droplets. Lastly, digitization of these assays increases processing times and can require custom or complex equipment and methods, making their use in point-of-care settings more challenging. Future work to address these challenges promises to transform the next generation of molecular diagnostic sensors, leveraging the significant advantages of digital assays.

Chapter 2: Sensitive and Stable Nucleic Acid Amplification with Cell-phone Based Readout

Nucleic acid amplification tests have primarily been limited to lab settings because of their complexity and relatively high costs. These tests have several advantages because of their unique capability to amplify DNA or RNA by at least a million-fold, enabling detection of a very small amount of target molecules associated with disease or the presence of microorganisms. Key challenges with point-of-care (POC) nucleic acid tests include achieving a low cost, portable form factor, and stable readout, while also retaining the same robust standards of benchtop lab-based tests. We addressed two crucial aspects of this problem, identifying a chemical additive, hydroxynapthol blue (HNB), that both stabilizes and significantly enhances intercalator-based fluorescence readout of nucleic acid concentration, and developing a cost-effective fiber optic bundle-based fluorescence microplate reader integrated onto a mobile phone. Using loop mediated isothermal amplification (LAMP) on lambda DNA we achieve a 69-fold increase in signal above background, 20-fold higher than the gold standard, yielding an overall limit of detection (LoD) below 57 copies/μL within an hour using our mobile phone based platform. Critical for a point-of-care system, we achieve >60% increase in fluorescence stability as a function of temperature and time, obviating the need for manual baseline correction or secondary calibration dyes. This field-portable and cost-effective mobile phone based nucleic acid amplification and readout platform is broadly applicable to other real-time nucleic acid amplification tests by similarly modulating intercalating dye performance, and is compatible with any fluorescence based assay that can be run in a 96-well microplate format, making it especially valuable for POC and resource-limited settings.

2.1 Introduction

Nucleic acid detection assays are used ubiquitously in medicine, from identifying viral or bacterial pathogens[32,33] to assaying for minimal residual disease in leukemia[34] and measuring unique sequences of circulating DNA to identify drug treatable mutations[35]. Point-of-care (POC) nucleic acid assays can provide advantages when a rapid readout or diagnostic decision is needed (e.g. for infectious diseases) or when assays need to be performed in a limited resource or distributed setting[36–38]. These settings and need for operation by unskilled users impose unique challenges for POC assays, related to cost, ease-of-use and accuracy[39,40]. POC nucleic acid detection assays require several key components including amplification, signal generation and signal detection methods to achieve sensitive and specific diagnostics. Amplification of nucleic acids is critical to increase the signal for a specific nucleic acid sequence.

A host of new nucleic acid amplification approaches have been developed with characteristics suited to point-of-care assays, including e.g. rolling circle amplification, helicase-dependent amplification, nicking endonuclease signal amplification, isothermal strand displacement amplification, among others[41,42]. A key characteristic that many of these assays, such as LAMP, share is decreased sensitivity to temperature fluctuations and/or isothermal operation[20,43]. Currently, POC isothermal temperature control has been achieved using low cost approaches. Examples include phase-change materials and either Mg-Fe alloy or CaO and water to generate heat with an exothermic reaction[40,44]. More recently, photonic heating has been used for precise control with minimal instrumentation[45,46]. LAMP has several advantages, including isothermal operation, and the ability to produce large amounts of amplified DNA product in a short amount of time with a single type of enzyme[47,48]. Additionally, the reaction and readout can take place in a single volume as a homogeneous “one-pot” assay, making it suitable for a POC setting. We focus on LAMP here, although several other amplification techniques could benefit from the

methods introduced. Following amplification, the presence of nucleic acids is predominantly measured optically.

Two general methods for generating an optical signal after amplification are (i) by directly measuring the amplified nucleic acid product and (ii) by indirectly measuring the depletion or generation of other reaction components. Current direct nucleic acid detection dyes include intercalating dyes and custom sequence-specific probes. Custom probes can be multiplexed in a single reaction, but they lack the universality of intercalating dyes, requiring careful design for each new assay, and can be costly. Intercalating dyes can provide a large signal when added to a nucleic acid solution following an amplification reaction; however, for a POC assay, the simplicity of a "one-pot" homogeneous assay is preferred, where the dye is present at the beginning of the reaction. Intercalating dyes such as SYBR Green, Ethidium Bromide, Acridine Orange, and even EvaGreen are all known to interfere with the nucleic acid amplification process, and lead to diminished amplified product when added prior to the start of the reaction[49–52], and delayed times for reaction completion. Alternatively, one can measure decreasing amounts of reactants or alternative products as amplification proceeds, such as in the case of using HNB as an indicator. HNB has been reported as a colorimetric metal ion indicator that changes color from sky blue to violet in the presence of Mg^{2+}. The generation of pyrophosphate during nucleic acid polymerization sequesters magnesium in solution, such that HNB-based sensing of Mg^{2+} has been shown to provide an accurate measurement of the extent of nucleic acid amplification[53,54]. However, subtle color changes are difficult to quantify at the same level of sensitivity as fluorescent markers/probes. Alternatively, electronic readout of pH changes has also been proposed as a marker of amplification[55,56], in which an unbuffered assay system is used. Buffering of the reaction solution in LAMP allows compatibility with a variety of sample matrices suitable for the POC. However, in a buffer-free reaction the no-template control run in parallel will often

not represent the same reaction conditions as the sample with matrix, potentially leading to calibration errors. Additionally, a non-standard cartridge is required to both run and read the assay when utilizing a pH semiconductor system to amplify and detect DNA.

Another key element for a distributed POC diagnostics platform is that the readout method needs to be cost-effective, compatible with standard laboratory assay plasticware, such as well plates, and easy to operate. Mass produced consumer electronics, such as smartphones, now have sophisticated optical components and computational processing power making them ideal candidates for designing advanced, extremely cost-effective, field-portable biomedical measurement tools[57,58] and have already been utilized by us and others to readout signals from immunoassays[59,60] and nucleic acid amplification reactions[61]. There is even strong commercial interest (e.g. Biomeme) in developing POC-based readout of nucleic acid amplification with standard thermocycling techniques[38]. However, there have not been any publications describing the approach to couple the low fluorescence intensity of samples with a mobile phone or studies using this system to measure nucleic acids.

Here, we present two innovations towards enabling highly sensitive and stable fluorescence-based quantification of isothermal nucleic acid assays in a well-plate format using a cost-effective and field-portable handheld reader that is integrated onto a smartphone. We discovered a new method to significantly enhance fluorescent nucleic acid intercalating dye performance by including HNB into the reaction mix, yielding greater than 20 times higher fluorescent signal change over background compared to current intercalating dyes without interfering with the nucleic acid amplification process. When compared to HNB alone as a colorimetric indicator of reaction progress, the improvement in signal over background was over 250 times. This novel chemistry significantly reduces the technical challenge to readout fluorescence signals resulting from the assay and provides a bridge to enable readout and

quantification with a novel mobile phone based fluorescent 96-well plate reader without special temperature or environmental control, providing an excellent match to the needs of POC settings. Using LAMP, this unique chemistry and detection platform provided significantly improved results compared to a commercial benchtop fluorescence plate reader with standard intercalating dyes. Both the novel dye system and portable reader provide significant advances for distributed nucleic acid based diagnostics in POC or field-settings using LAMP or a range of other nucleic acid amplification approaches.

2.2 Results and Discussions

2.2.1 Enhancing Intercalating Dye Performance with Hydroxynapthol Blue

Although HNB is often used as a colorimetric indicator of nucleic acid amplification alone, we found that it interacts with intercalating dyes to lower the fluorescence background signal and significantly enhance the signal fold change during amplification. Real-time LAMP was run with HNB dye alone, in combination with EvaGreen, and EvaGreen without HNB. The chemical structures of EvaGreen and HNB can be found in **figure 2.1a** and **figure 2.1b**, respectively. Both reactions were conducted using the same conditions and measured for 2.5 hours. In **figure 2.1c**, the maximum fold change from the initial fluorescence at time zero was approximately 3-fold in the 1.25 μM EvaGreen concentration. However, when HNB was added, the maximum fold change increased to 20-fold (**figure 2.1d**). Even higher EvaGreen concentrations, that normally completely inhibit the nucleic acid amplification, were also investigated and found to generate fold changes as high as 69 (**figure 1f**, **appendix A. figure 2**). Reactions containing only HNB for colorimetric detection are shown in **appendix A. figure 3** where absorbance was measured. For HNB alone, the signal is delayed in time and only increased about 20% above the baseline value following amplification. For further experiments reported in this manuscript we chose to use 1.25

μM EvaGreen combined with 120 μM HNB which gave a sufficiently increased signal fold change (20-fold) while minimizing reagent costs. As with all nucleic amplification techniques, LAMP is not immune to non-specific amplification, as seen in the zero DNA cases after 100 min in **figure 2.1c and 2.1d**.

These results reveal that the addition of HNB was found to interact favorably to limit the inhibitory effects of the addition of an intercalating dye on the DNA amplification process and reduced the time to amplification. For all reactions with HNB added to the solution, the time to double the initial fluorescence intensity is significantly less than for the reactions without HNB (**figure 2.1e**), suggesting that the inhibitory effects of intercalators, like EvaGreen on polymerase activity[49–51] is mitigated by the presence of HNB. With increasing amounts of EvaGreen without the presence of HNB, the time to double the fluorescence increases dramatically, and above 2.5 μM EvaGreen, the reaction is so slow that doubling in intensity is not achieved within the 3.5 hr cutoff of our experiment. However, when HNB is added to the reaction mix, the time to double fluorescence intensity remains steady at less than 40 minutes up to the highest concentration of EvaGreen tested (6.25 μM).

In addition to increasing the signal and reducing the amplification time of our assay, the presence of HNB in the reaction solution was also found to allow for an increased temperature stability of the fluorescence intensity of the intercalating dye. Decay in the fluorescence intensity of EvaGreen over time is apparent in the reaction without HNB (**figure 2.1c**). The fluorescence decays over time from a maximum at time zero, when the reaction is held at 65 °C, even for the negative control without polymerase. For the negative control, the fluorescence decays approximately 75% from its maximum value at time zero in the case without HNB, and between 4-12% when HNB is present in solution (**figure 2.1d**). This suggests that the interactions between HNB and EvaGreen act to diminish photobleaching and/or temperature effects on dye

conformation or degradation over an extended time. These results suggest a strong interaction between HNB and the intercalating dye might be leading to the beneficial properties. Importantly, this reduced baseline drift eliminated the need for inclusion of separate normalization dyes or manual baseline correction that is often performed in commercial nucleic acid amplification readout[62,63].

We next identified that HNB interacts more generally with intercalating dyes to improve the dye performance. We observed that HNB also provided beneficial effects when combined with other intercalating dyes such as SYBR Green and Acridine Orange to enhance the readout of LAMP with these dyes present (**appendix A. figure 4**). The temperature stability for SYBR Green and Acridine Orange were both increased in the presence of HNB, however, the effects on temperature stability for Acridine Orange was more pronounced. In addition, the increase in fold change of fluorescence above the reaction start time was markedly increased for Acridine Orange (rising from 2-fold to 5-fold) compared to SYBR Green (2-fold to 3-fold). Since EvaGreen consists of a dimer of Acridine Orange, these results suggest that although HNB interacts with other intercalating dye structures, the interactions with Acridine Orange are particularly favorable.

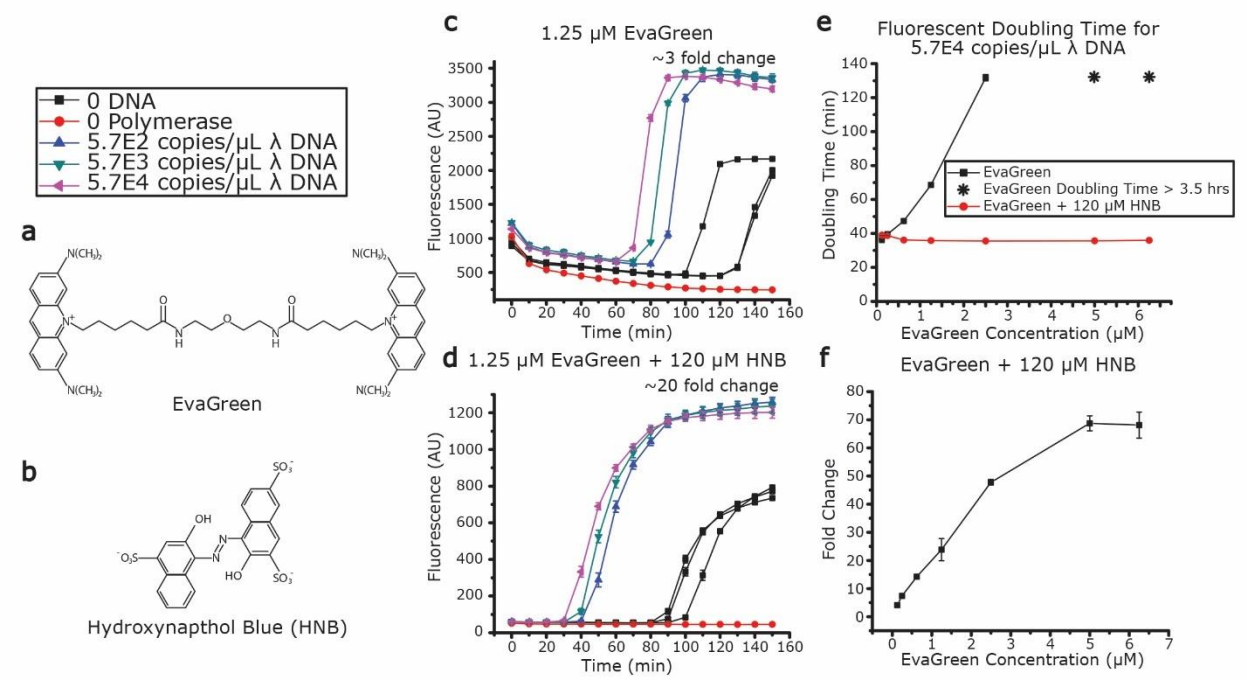

Figure 2.1 *Chemical structures of a. EvaGreen and b. Hydroxynaphthol Blue (HNB); Real-time fluorescence measurements of λ DNA amplification with loop-mediated DNA amplification (LAMP) with c. 1.25 µM EvaGreen d. 1.25 µM EvaGreen and 120 µM HNB. Each replicate of the 0 DNA condition is shown separately as this condition is prone to contamination. e. The time to reach 2-fold of the initial fluorescence for each EvaGreen concentration tested both with and without HNB. f. The overall fold change (150 min/0 min) for each EvaGreen concentration tested with 120 µM HNB. All error bars indicate s.d.*

Temperature stability is essential in assays developed for POC or field use, and HNB was observed to interact directly with EvaGreen to stabilize the fluorescence intensity with changes in temperature even without the presence of DNA in solution. In order to examine the interactions between EvaGreen and HNB directly, the fluorescence intensity of a solution of EvaGreen without DNA in DI water was measured over temperature cycles and compared with the same solution with added HNB. **Figure 2.2a** shows that with increasing temperature, the fluorescence decreases in the solution without HNB, whereas, the fluorescence of the solution with HNB increases with temperature. The solution without HNB displays hysteresis, with the fluorescence dependent on the direction of the temperature cycle. Additionally, the range of fluorescent intensities is much

larger in solution without HNB (6000-11000 AU) versus (1800-2800 AU) in the solution with HNB. Overall, the temperature-induced changes in fluorescence are much greater when HNB is not present in solution with EvaGreen. This large instability with temperature using EvaGreen alone makes it more difficult to interpret changes in fluorescence as a result of DNA amplification from changes due to temperature fluctuation. The ability for the fluorescence to remain stable across a range of temperatures is especially important in point-of-care or low-resource settings. Since the overall fluorescence of EvaGreen decreases with the presence of HNB, this could further indicate that the blue dye attenuates excitation/emission light and/or interacts with EvaGreen in solution to reduce effective quantum yield of the dye. The fact that intensity of EvaGreen increases with ramping temperature, while decreasing in a non-recoverable fashion without HNB, suggests that the latter is at least partly true. Increased entropic contributions at higher temperature would favor dissociation of a EvaGreen:HNB complex and increased quantum yield. Therefore, HNB and EvaGreen most likely directly interact in solution, and HNB modulates the fluorescence intensity and stability of EvaGreen.

The temperature stability of the HNB-modified assay has several advantages for endpoint readouts that make it compatible with POC or low-resource systems. In figure 2b and c we evaluated the effect of the addition of HNB on fluorescence signal changes following nucleic acid amplification. We measured at time 0 before amplification and heating, and at warm (55 – 65 °C) and room temperature (20-25 °C) conditions following amplification. Without HNB, for all concentrations of λ DNA, the endpoint (40 min) fluorescence intensity is less than the initial fluorescence intensity at room temperature, which would require a separate control well to normalize for intensity fluctuations of the dye alone. Still using a 0 DNA control as the negative condition leads to a poor limit of detection when reading warm plates, and an even further reduced LoD when reading the plate following cooling to room temperature. In the case where HNB is

added to the reaction mix (**figure 2.2c**), not only is the endpoint fluorescence significantly higher than the initial fluorescence for λ DNA concentrations higher than 5.7E3 copies/µL, but even after cooling to room temperature, this difference between λ DNA concentrations can still be discerned.

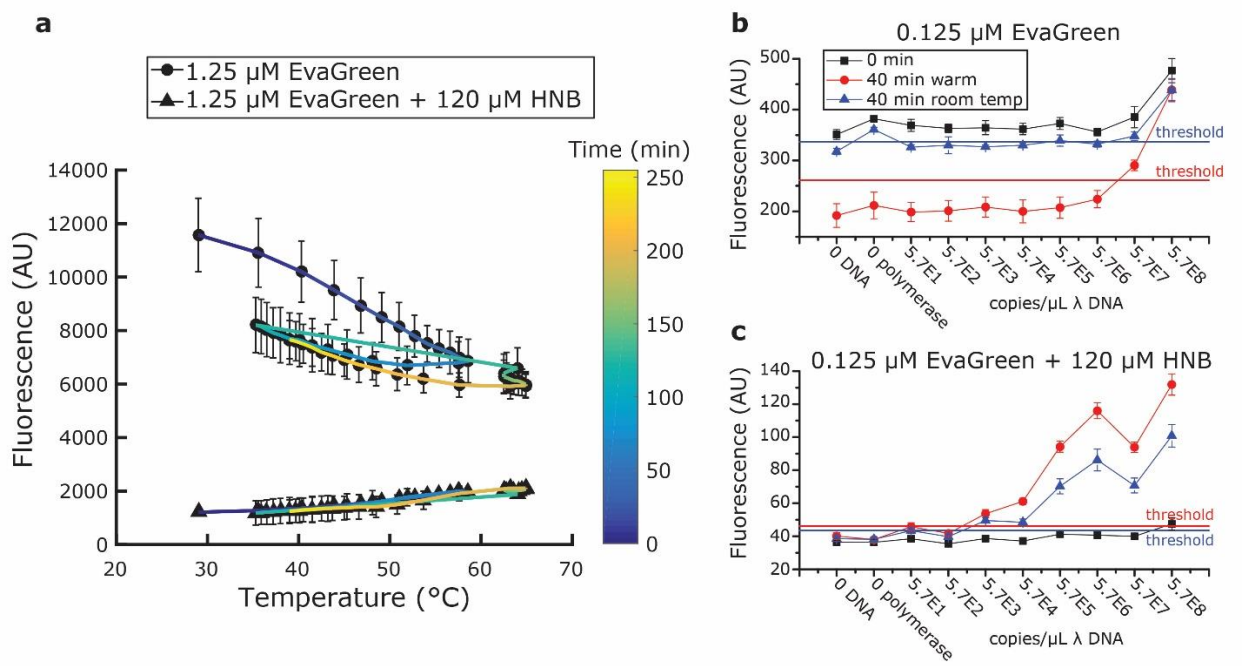

Figure 2.2. *a. Fluorescence measurements taken over temperature cycles ranging from 29-65 °C for EvaGreen and EvaGreen with HNB in DI water; Initial and endpoint fluorescence measurements taken with a benchtop plate reader of λ DNA amplification with loop-mediated DNA amplification (LAMP) with b. 0.125 µM EvaGreen and c. 0.125 µM EvaGreen with 120 µM HNB. The warm condition is when the plate is measured immediately following the reaction (approximately 55-65 °C). The room temp condition is taken after the plate has reached room temperature (approximately 20-25 °C). Threshold values shown as horizontal lines are defined as the fluorescence of 0 DNA plus 3 standard deviations. All error bars indicate s.d.*

Having identified HNB as a simple additive to a nucleic acid amplification assays that would allow for a one-pot reaction with significantly increased fold signal above background and increased temperature stability useful for POC diagnostics, we next focused on developing and integrating this assay with a cost-effective mobile phone based fluorescence well-plate reader, to achieve a more complete solution for nucleic acid amplification based POC tests. When developing assays for POC settings, mobility and ease of use are key. The addition of HNB in the

assay allows for a one-pot system, removing the need for several steps and improving ease of use. HNB addition improves the signal above background as well as shortening the time to reach a detectable signal. Lastly, HNB provides stability in the fluorescence signals over a large range of temperatures, which is crucial in environments where temperature cannot be as closely monitored. To further achieve a more complete POC solution, we created a mobile phone based plate reader which is not only more cost-effective than standard benchtop fluorescent plate readers (~$50,000), but is also field-portable while achieving comparable results against its benchtop counterpart, as will be detailed next.

2.2.2 Mobile Phone Based Fluorescent Plate Reader Performance

Our mobile phone based fluorescent plate reader device is assembled via exchangeable 3D-printed parts (**figure 2.3a**). The compactness of this fluorescence reader platform that images a large sample field of view of ~18 cm^2 is achieved by using an optical fiber bundle to map the fluorescence signal of 25 wells onto a small area (dia ~10 mm) in front of the cellphone camera (**figure 2.3b**). This fiber bundle, together with the fluorescence imaging system formed by the cellphone lens and an external lens, create a total demagnification factor of >13 within a very compact design, where the overall height of the device is <10 cm (**figure 2.3c and d**). In a single image, without any mechanical scanning this handheld device can read an array of 5x5 = 25 wells of a conventional 96-well plate all in parallel (figure 3e, right); quite conveniently the plate can be inserted into the device in either direction, which means 50 wells of the same plate can be measured in two successive measurements. At the bottom of each well, three optical fibers (0.4 mm dia. each) are mounted, and at the other end of the fiber bundle, the optical fibers are randomly grouped. A look-up map of fiber location versus the well position was established before the actual experiments, which only needs to be performed once per device design. **Figure**

2.3e shows a representative fiber pattern captured on the mobile phone reader, where only 7 of the 25 wells were randomly loaded with fluorescein solution. This unique design has significant advantages: (1) the fiber bundle helps us achieve a cost-effective, compact and light-weight fluorescence imaging design with a large demagnification factor so that a wide sample area of ~18 cm^2 can be imaged without the need for any mechanical scanning or bulky optics; and (2) each one of the three fibers per well experience different amounts of spatial aberrations, noise as well as losses and their averaging minimize well-to-well variations of our design. Although we focused on blue excited, green emission fluorescent dyes that cover a wide range of intercalators and DNA probes in this work, the multimode optical fibers are compatible with a wide range of wavelengths, and by appropriately selecting the excitation/emission filters and LEDs, the same platform can easily be adapted for digital readout and quantification of various fluorescent and colorimetric assays.

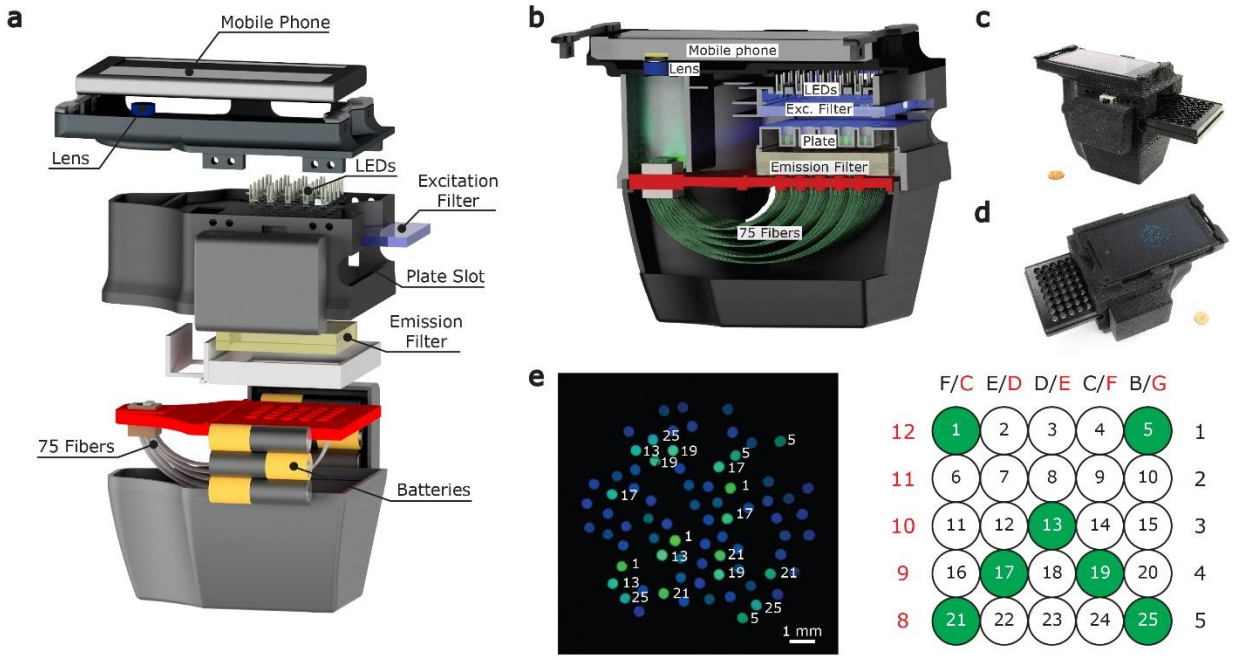

Figure 2.3. *Design of the mobile phone fluorescence plate reader device. a. Anatomy of the mobile reader device. b. Schematic side view showing inner structure. c.,d. Real photographs of the device. e.*

Representative mobile phone fluorescence image of the random optical fiber pattern, and corresponding well positions on the right.

The performance of each well of our mobile reader device was calibrated against the readings of a conventional benchtop plate reader (**appendix A. figure 5a**), which reads each well in a serial manner, i.e., using a mechanical scanning system. As detailed in the Methods section, following image format conversion, segmentation, and intensity averaging from 3 fibers, a normalization factor was obtained by dividing the mean mobile phone intensity reading by the corresponding benchtop fluorescence reading (**appendix A. figure 5a**). For example, the red circles in **appendix A. figure 5b** represent a set of normalization factors for the first well position only, which is superimposed on its fitting curve (black), together with the rest of the calibration curves for the remaining 24 wells in the background. **Appendix A. figure 5c** shows the comparison between the conventional benchtop plate reader measurements (Biotek) and our mobile phone fluorescent plate reader. After proper calibration and normalization, a series of diluted fluorescein solutions were blindly tested for each well position of the mobile reader device. Based on linear regression between the mobile phone intensity readings and the dye concentration in the range of 0-10 nM, the LoD was determined by a threshold of three times the standard deviation of the blank control samples added to their mean (**appendix A. figure 6a and b**). Our results illustrate that all 25 well positions showed a LOD of <1 nM fluorescein with a mean LoD of 0.18 nM (**appendix A. figure 7**).

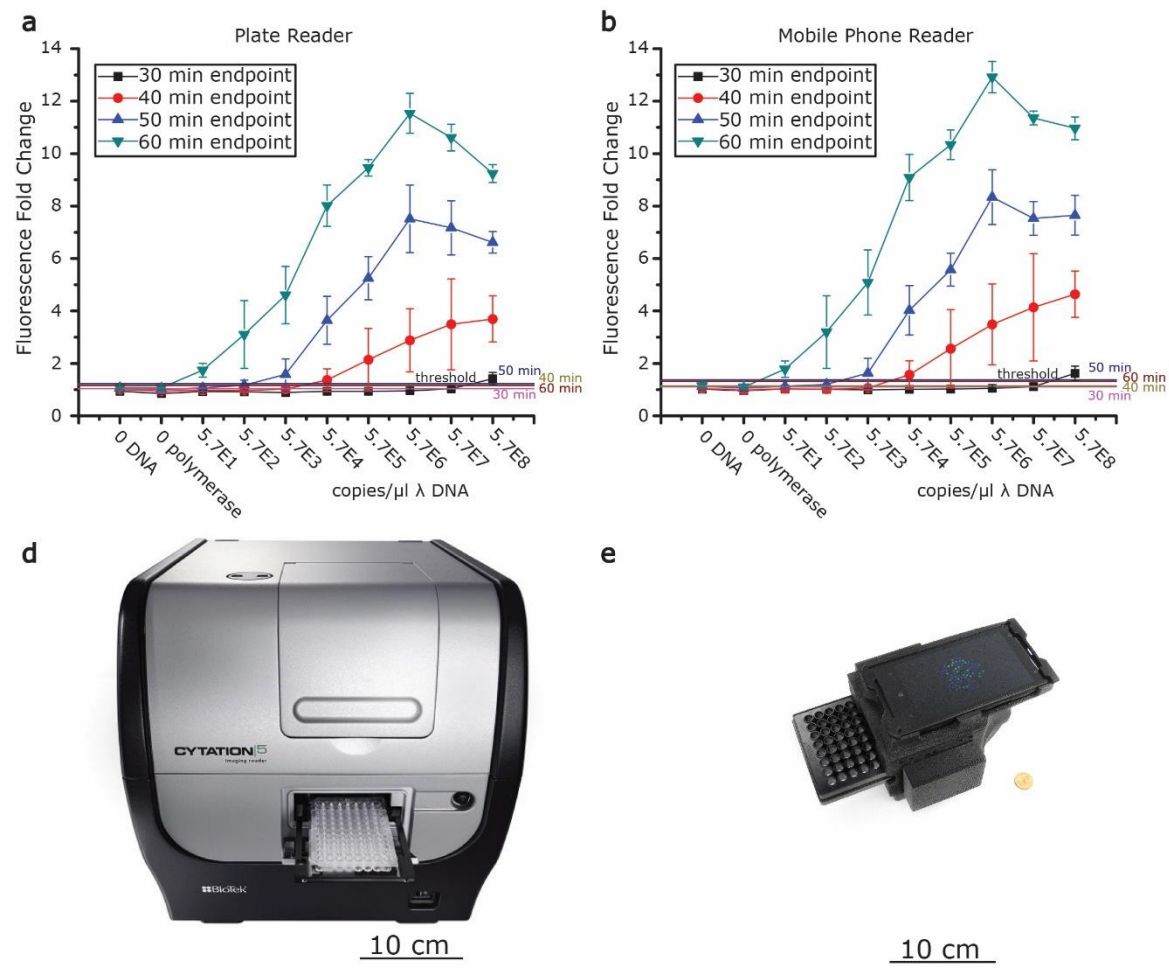

Figure 2.4. *Normalized fluorescence to 0 DNA for 30, 40, 50, and 60 minute assays when imaged with a. a benchtop plate reader and b. mobile phone reader. Colored threshold values for each endpoint are shown as horizontal lines and are defined as the mean 0 DNA fluorescence value plus 3 standard deviations; c. Biotek Cytation 5 benchtop plate reader used as the gold standard d. novel 25-well mobile phone reader, suitable for point-of-care (POC) settings. All error bars indicate s.d.*

After establishing the LoD of our mobile fluorescent plate reader, next we applied it to analyze signals from enhanced LAMP reactions that included HNB. Comparing the fluorescent fold changes for both the benchtop plate reader and our cell phone based design (**figure 2.4**), we can clearly see that the trends match and the concentrations of λ DNA that can be distinguished above background are the same for both the benchtop plate reader and the POC mobile phone-based reader. For both systems the fluorescence fold change measured above background is significantly elevated with the HNB additive compared to a LAMP reaction alone, which results

in a lower limit of detection. The amount of DNA amplification that occurs during the assay is dependent on the length of time the assay runs. As such, the longer the assay is run, the lower initial λ DNA concentration is needed in order to generate a signal above baseline. This leads to a lower LoD with an increased assay runtime, as shown in **figure 2.5**. After 60 minutes, the mobile phone based assay can detect as few as 127 copies/μL λ DNA which approaches the limit of detection of approximately 11 copies/μL DNA reported[64], which was performed in a laboratory setting. Therefore, our system can detect a similar amount of DNA using techniques suitable for POC or low-resource settings. In fact, the ability to amplify DNA from ~100 copies/μL level is sufficient to detect a wide range of disease states, microbial populations, or rare gene mutations. For example, meningococcal bacterial DNA load in patients ranges from 22 – 1.6E5 copies/μL, with the median being 1.6E3 copies/μL[65].

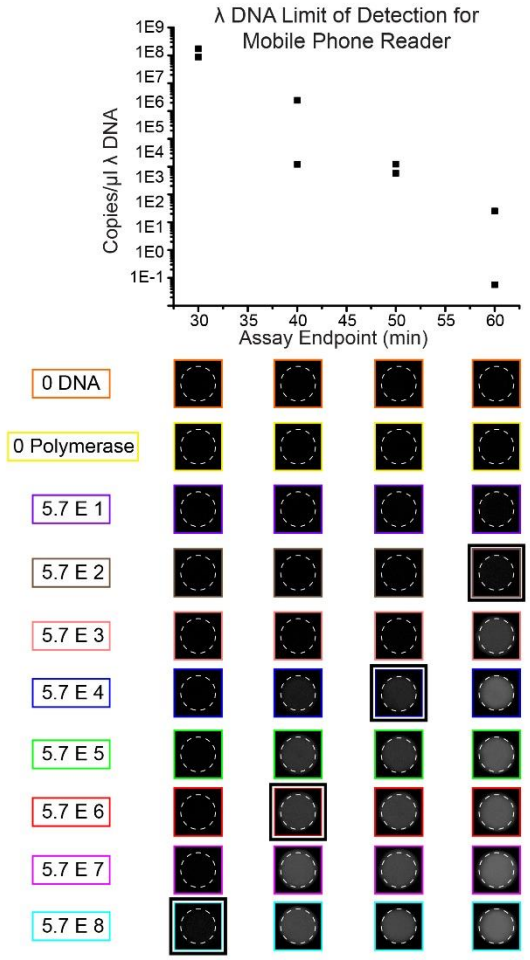

Figure 2.5. The limit of detection (LoD) of λ DNA when using the LAMP assay and measuring fluorescence with the mobile phone reader following amplification for increasing amounts of time up to 60 minutes. Characteristic fiber images of each of the λ DNA concentrations are shown below each of the corresponding endpoints with the LoD highlighted with a black outline.

2.3 Conclusions

We have presented two key techniques that can be used to significantly improve upon current POC nucleic acid based assays. We demonstrated that HNB interacts favorably with intercalating dyes, increasing temperature stability and decreasing temperature-dependent decays in fluorescence, while simultaneously decreasing interference with the amplification process and

allowing for the change in fluorescence intensity to be visualized earlier and with greater fold changes. These unique interactions allow for this dye combination to be added prior to the start of a reaction, providing a system where the reaction can be measured in real time, but also simplifying the assay steps and decreasing the risk of contamination across samples. Not only is the signal generated greater with the addition of HNB, but the signal is more stable with temperature changes, enabling measurements at POC or low-resource settings after the reaction has completed and cooled to room temperature. Replacing an intercalating dye or probe for this dye combination is a simple step to integrate with any number of nucleic acid amplification processes, including qPCR, rtPCR, and several other isothermal amplification techniques such as nucleic acid sequence-based amplification (NASBA) or the proximity ligation assay[66,67]. The universality of this dye combination allows for its use in any nucleic acid assay without the need to design custom and costly nucleic acid probes. Another benefit of this system is that the high signal generated can be easily integrated into digital DNA amplification protocols, which typically have a low signal to background ratio between 2 and 6.5[24], even after the use of a reference dye.

In addition to significantly improving the signal strength and stability for general nucleic acid amplification tests, we also developed a field-portable, cost-effective and lightweight instrument that can easily sense this enhanced signal in a POC-friendly manner. Our mobile phone based fluorescent well plate reader can not only be operated in a POC setting but also can be easily integrated with existing standard well plate formats and materials for nucleic acid assays. Notably, the combination of the mobile phone based reader and dye mix requires no baseline corrections or reference dyes such as ROX to normalize results like in many other nucleic acid amplification systems, leading to a simpler and lower cost solution that does not require multiple wavelength readout. We have presented improvements on two aspects that can be used to improve current POC assays, but further challenges should be addressed for a completely integrated solution. Sample

preparation steps and their integration with our assay will need to be addressed. We were able to demonstrate how the assay would work with a purified sample of λ DNA, but further validation with more complex sample matrices, such as blood plasma, sputum, and other bodily fluids is needed. Currently, the well plates need to be heated in an oven that is held at 65 °C, but POC isothermal heating can be achieved using a number of approaches, including e.g., exothermic chemical reactions and phase changing materials[40,44]. Additionally, reagent storage is currently at -20°C and 4°C, but in order for the system to be compatible with POC settings, long-term reagent storage conditions will need to be addressed. Further testing needs to be done to see if the reagents can be lyophilized and stored at room temperature[42,68–70]. As with most nucleic acid amplification techniques, contamination is always a concern[71]. However, in POC settings the risk of contamination is lessened because the target DNA will not be present in as high quantities as a testing facility that continually produces amplified target DNA product.

The enhancements achieved from the techniques demonstrated here should also be compatible with digital nucleic acid amplification tests that make use of arrays of sub-nanoliter volumes in order to provide single-molecule counting. Signal to noise in digital LAMP systems is typically very low, between 2 to 6.5[24], and this range is only achieved after the use of a reference dye to remove background. The addition of the combination of EvaGreen and HNB to digital LAMP systems may be able to improve accuracy of detection with lower cost optical systems by decreasing the overall background signal and mitigating the inhibitory effects of the presence of an intercalating dye on reaction progress. In summary, we have shown that the mobile phone based reader provides comparable fluorescence quantification results to a standard benchtop plate reader, and when combined with the intercalator sequestering approach this unique POC platform achieves significantly enhanced performance compared to a benchtop reader with standard LAMP conditions.

2.3 Materials and Methods

2.3.1 LAMP Assay

All components of the assay reaction mixture were purchased from Sigma, and all primers were purchased from Invitrogen unless otherwise stated. LAMP reaction buffer consists of 20 mM Tris-HCL (pH 8.8), 10 mM KCL, 10 mM ammonium sulfate, 8 mM magnesium sulfate, 1 M Betaine, 0.1% Triton-X 100, and 1.6 mM dNTPS (Invitrogen) in ultrapure DNAse/RNAse free water (Invitrogen). The LAMP reaction was carried out in 100 µl volumes on a 96-well plate in triplicates for time-course readings, and in 5 wells for end point readings. 10 µl of serially diluted λ DNA (Thermo Fisher), 0.64 µM FIP and BIP, 0.08 µM F3 and B3, 0.16 µM Loop F and Loop B, 32 units Bst DNA polymerase large fragment (New England Biolabs), 120 µM HNB, and varying amounts of EvaGreen (Biotium) were added in the LAMP reaction buffer. In the case where other fluorescent intercalating dyes were used, SYBR Green (Invitrogen) and Acridine Orange, the concentrations used are stated. Two negative controls, 0 DNA and 0 DNA w/o polymerase were used. Two negative controls were used because of the high risk for contamination from neighboring wells with high levels of amplification. Real-time fluorescence measurements were taken in duplicate for triplicate wells using a Biotek Cytation 5 plate reader set at 65 °C for 2-2.5 hours. For the experiment comparing warm and room temperature plate readings, single point measurements in triplicate wells were taken using the mobile phone reader and the Biotek Cytation 5 plate reader, and the plates were heated at 65 °C using an oven for 40 minutes. For limit of detection experiments, three replicate intensity measurements from 5 wells with each concentration were taken at the experiment endpoints. The average fluorescence intensity corresponding to each concentration and endpoint is calculated by averaging 15 measurements (3 replicate measurements of 5 wells). The lowest concentrations of 5.7E-1 and 5.7E0 copies/µL were

only examined for the 60-minute endpoint. The threshold for a positive reading above background is defined as the fluorescence intensity of the 0 DNA plus three standard deviations at that endpoint. The LoD for each experiment was calculated by interpolating a threshold DNA concentration from the two sequential measured concentrations that were above and below the threshold. The LoD is determined to be the concentration at the intersection between the fluorescence threshold and a line connecting the points one standard deviation below tested concentrations above and below the threshold. If for the concentrations tested, no average minus one standard deviation fluorescence intensities fell below threshold, the lowest concentration tested was used as the LoD for that experiment. The LoD shown in figure 5 was calculated by averaging the LoD for replicate experiments. To validate the mobile phone fluorescence plate reader, all the measurements taken with the mobile phone were also repeated using a Biotek Cytation 5 plate reader, used as our gold standard. All measurements were taken at room temperature. We report the raw data from the plate reader for all data shown. This is notably different than standard qPCR instruments that include manual calibrations and corrections for baseline drift, which often require additional dyes and readout wavelengths (e.g. ROX-based calibration) that is difficult to implement in a POC device.

LAMP Primers:

FIP: CAGCCAGCCGCAGCACGTTCGCTCATAGGAGATATGGTAGAGCCGC

BIP: GAGAGAATTTGTACCACCTCCCACCGGGCACATAGCAGTCCTAGGGACAGT

F3: GGCTTGGCTCTGCTAACACGTT

B3: GGACGTTTGTAATGTCCGCTCC

Loop F: CTGCATACGACGTGTCT

Loop B: ACCATCTATGACTGTACGCC

2.3.2 Temperature Studies with EvaGreen and HNB

Solutions containing 1.25 μM EvaGreen in DI water and 1.25 μM EvaGreen with 120μM HNB in DI water were fluorescently measured over temperature cycles. The initial temperature cycle starts from 29 °C, and the fluorescence intensity was tracked over a range of temperatures up to 65 °C. Two fluorescent measurements of triplicate wells were taken using a Biotek Cytation 5 plate reader.

2.3.3 Cell-phone based portable fluorescent microplate reader

We prepared a mobile phone based fluorescence plate reader by integrating a custom-designed 3D printed opto-mechanical interface with the camera module of a smartphone (Nokia Lumia 1020). In our 3D printed optical interface, an array of 5x5 blue LEDs (470 nm, DigiKey) was mounted above the plate and used as the excitation light source for fluorescence. Excitation (465/30 nm, OD 6, 50x50 mm, Semrock) and emission (530/30nm, OD 6, 50x50 mm, Omega Optical) filters were placed above and below the disposable plate, respectively, and fluorescence signal was collected from the transparent floor of each well by three individual multimode optical fibers (dia. 400 μm core, FT400UMT, Thorlabs) that are all placed at a plane that is parallel to the well plate. A total of 75 fibers (3 fiber-optic cables per well, and 25 wells in total) were bent within the attachment, forming a circular common end with each fiber randomly bundled together. This fiber common end, composed of 75 individual fibers, was then imaged by the smartphone camera via a single lens (f = 15 mm, Edmund Optics) that forms an imaging system together with the

existing lens of the smartphone with a demagnification factor of ~2.2. Excluding the mobile phone, this entire fluorescent reader platform weighs < 600 g and its cost is estimated to be <100 USD not including the custom-fabricated large area optical filters, the cost of which can be reduced to <300 USD under large scale manufacturing. In a typical mobile phone based image acquisition experiment, an exposure time of 4 sec was used with an ISO of 100. The focus was set to infinity and images were saved in the raw DNG (digital negative) format. To minimize the autofluorescence background, black 96 well plates with clear bottoms (Corning) were used for all measurements.

2.3.3 Characterization of the Limit of Detection (LOD)

To characterize the fluorescence limit of detection of our mobile phone based reader, fluorescein solutions (0-50 nM) were loaded into the plate and imaged. The captured mobile images were first batch-converted to TIFF format single channel images (green channel for fluorescein) using ImageJ. A Matlab algorithm that can automatically locate individual optical fibers and measure their intensities was also developed. For each well, the intensities from three corresponding fibers were averaged and used as the intensity for that specific well. These average well intensities were then plotted against the concentration of fluorescein for each individual well, and linear fitting was performed within a concentration range of 0-10 nM. To better estimate the measurement errors, each plate for a given dye concentration was inserted, imaged, and removed for three independent cycles. The fluorescence LoD for each well was individually determined by the average signal of blank control (0 nM concentration) plus 3-timesits standard deviation. At the end of this process, the LoD was characterized for each well, and in total 25 LoDs were obtained.

2.3.4 Intensity Normalization of Wells

A computational framework was also developed to minimize small intensity variations from well to well due to the spatial variations of light intensity of LEDs as well as bending induced light transmission differences among individual optical fibers. In order to develop a normalization map, fluorescent well plates with varying intensity levels were imaged by both our mobile phone based reader and a conventional benchtop plate reader, used as the gold standard in our measurements. Then, a normalization factor (F) was obtained for each well and at each assay concentration by using the following equation:

$$\mathrm{F} = \frac{I_{cellphone}}{I_{plate\ reader}}$$

where $I_{cellphone}$ represents the raw intensity of the mobile phone based readout, and $I_{plate\ reader}$ represents the corresponding gold standard reading from a benchtop plate reader. Nonlinear curve fitting was then performed to the scattered plot of mobile phone raw intensity ($I_{cellphone}$) versus normalization factor (F) to form a normalization function for each well. Finally, normalized mobile phone intensities were obtained by dividing the mobile phone raw intensities by the corresponding normalization factors determined by the fitting functions. This normalization procedure was performed only once to determine the normalization function for each well and remained the same for the rest of the experiments.

Chapter 3: Digital Loop-mediated Isothermal DNA Amplification (LAMP)

The fluorescence emissions generated in a nucleic acid amplification are dependent on the fluorescence of the individual components of the assay as well as any complexes formed. In this work, we focused on determining the emission spectra of each component and complex formed, and determined when it is more favorable to form a complex between an intercalator and sequestration molecule versus an intercalator and a DNA molecule. By examining the absorbance and emission spectra of various intercalating dye and chemical additives, we were able to ascertain what effects they may have on the loop-mediated isothermal DNA amplification (LAMP) process that leads to signal improvement. Our studies showed that intercalating dyes such as EvaGreen, SYBR Green, and acridine orange have strong Förster resonance energy transfer (FRET) interactions, and this interaction leads to a decrease in the baseline fluorescence signal for solutions without DNA, measured at 535 nm. Additionally, when the absorbance and emission spectra for LAMP solutions with and without DNA are examined pre- and post-amplification, the binding kinetics, and the balance between the intercalating dyes, the chemical additive, DNA, and subsequent complexes are elucidated. We have found that EvaGreen and HNB interact in a manner that HNB sequesters the intercalating dye when there is only a small amount of DNA present, and after amplification, when there is a large accumulation of DNA, the EvaGreen binding shifts from the HNB to DNA and generates an increase in fluorescence signal. Understanding the mechanics of these dye interactions allow for further development, optimization, and discoveries for the addition of an intercalating dye and sequestration molecule to a nucleic acid amplification assay.

3.1 Introduction

Intercalating dyes are known to interfere with the amplification process[49–52], but as shown in chapter 2, we have identified a chemical additive to EvaGreen, hydroxynapthol blue (HNB), that has a mitigating effect on this interference, provide stability with temperature changes, and increased fluorescence fold changes. By examining the changes in absorbance and emission spectra, the mechanics of these interactions can be investigated. Not only was the spectra of the previously tested dye combination studied, but similar dye combinations were investigated as well to elucidate the differences in interactions and the roles that each has in altering the fluorescence over the course of the LAMP amplification reaction. By better understanding the mechanics of why this dye combination works, we can then apply this knowledge to other amplification techniques and work toward optimizing the fluorescence readout without interfering with the amplification process. The proposed mechanism for this interaction is shown in figure 3.1, prior to amplification, if an intercalator molecule is present is solution, the interaction with DNA will interfere with the amplification process. Whereas if a sequestration molecule is present, the molecule will sequester the intercalator, allowing amplification, and interacting via FRET to decrease the background signal. Once amplification occurs, the balanced for the binding kinetics shifts such that intercalator and DNA molecule complexes are more favorable, allowing for a fluorescence signal to be measured.

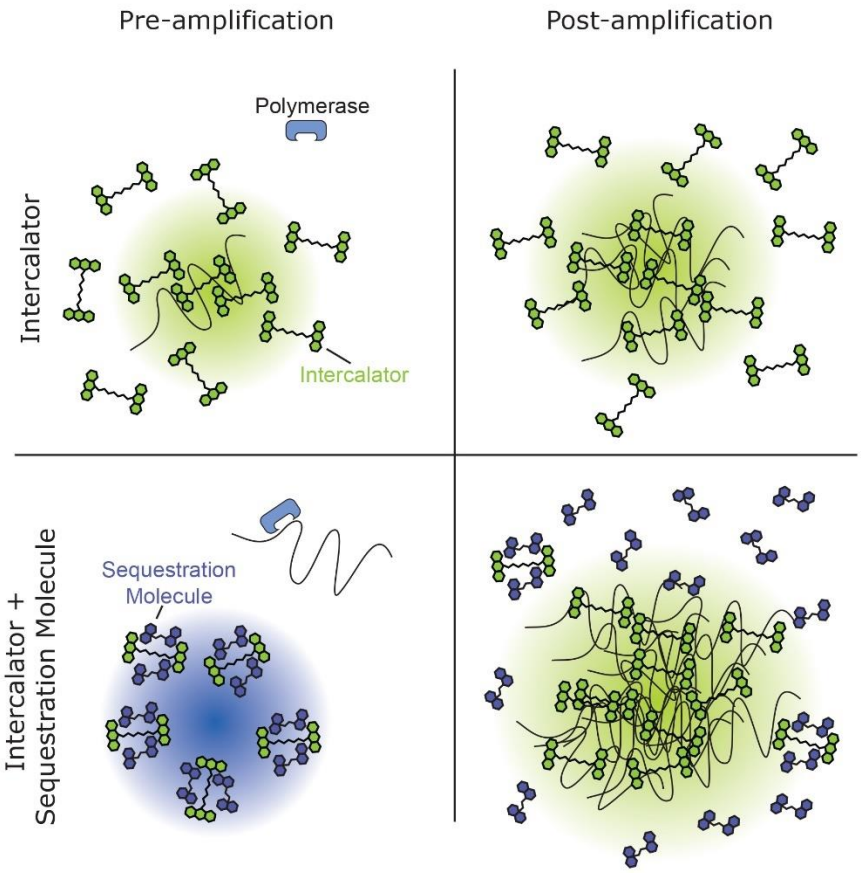

Figure 3.1. *Proposed mechanism of interaction between intercalating dyes and sequestration molecules.*

3.2 Results and Discussion

The emission spectra for various intercalating dyes were examined to compare the signal in the presence of DNA at 535 nm compared to the background without DNA (**figure 3.2**). While SYBR green shows the greatest fluorescence change, giving the highest signal to background, previous studies have shown that SYBR Green added prior to the amplification reaction greatly hinders the amplification process. The signal generated from the addition of DNA to acridine orange or EvaGreen is not drastically higher than the background, and in some cases, cannot be distinguished from the background. The absorbance and emission curves for 2.5 μM EvaGreen and 120 μM HNB in **figure 3.3** show that there is a significant amount of overlap between the wavelengths absorbed by HNB and the wavelengths emitted by EvaGreen. The temperature studies

conducted in chapter 2 demonstrated that even in the absence of DNA, EvaGreen and HNB interact in solution. These absorption and emission spectra suggest that this may be a FRET interaction. Comparing the emission spectra for the solution containing EvaGreen versus EvaGreen and HNB shows that the emission peak at approximately 535 nm is greatly reduced when HNB is present, and when DNA is added to the solution containing the dye combination, the emission at 535 nm increases significantly. This is suggestive that there is a balance for binding affinities between DNA and EvaGreen, and HNB and EvaGreen. This further suggests that the addition of DNA to the solution with both dyes alters the binding kinetics such that EvaGreen and HNB FRET interactions are decreased.

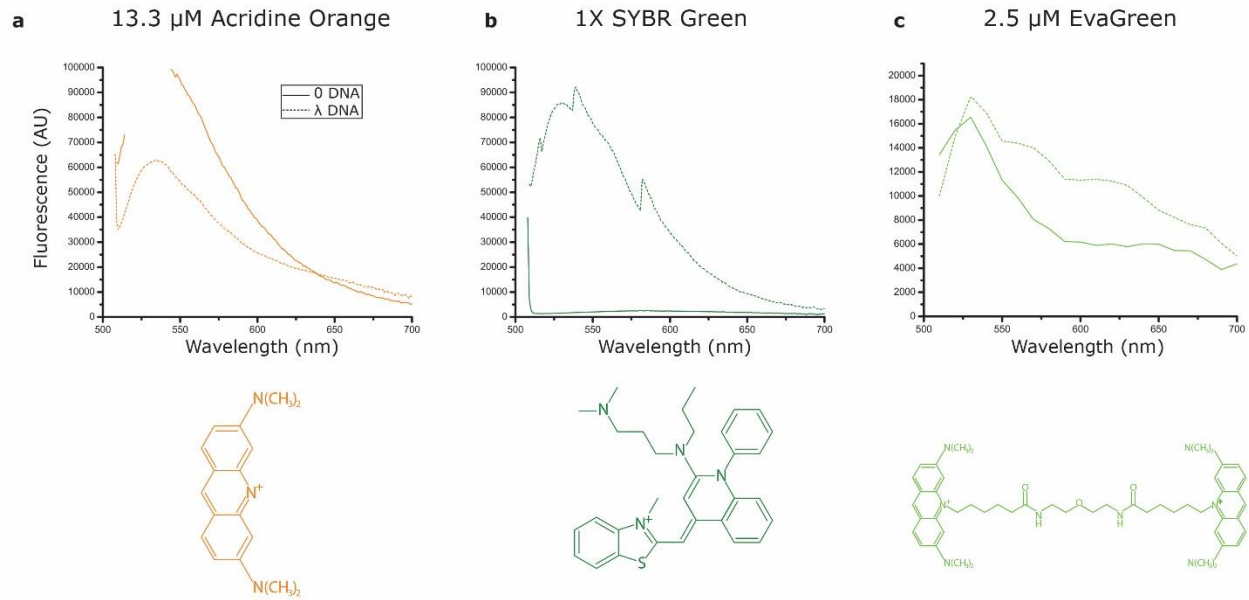

Figure 3.2. *Chemical structures and emission spectra with and without the presence of DNA for intercalating dyes a. acridine orange. b. SYBR Green and c. EvaGreen*

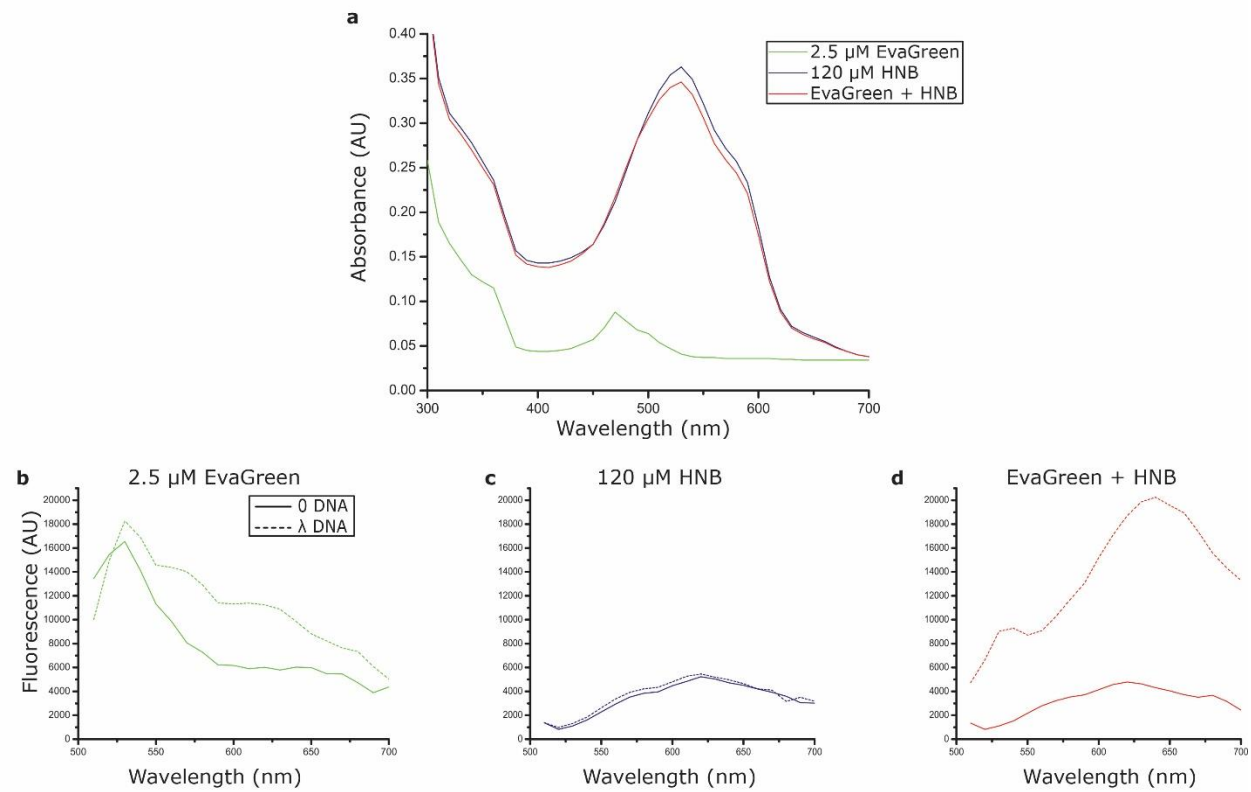

Figure 3.3. *a. Absorbance and emission spectra for b. 2.5 µM EvaGreen, c. 120 µM HNB and d. both 2.5 µM EvaGreen and 120 µM HNB with and without λ DNA*

Next, examining the absorption and emission spectra of the LAMP reaction can show the role of the reaction buffer and DNA amplification. The reaction buffer contains a high concentration of magnesium, which is known to change the absorption spectra of HNB[53]. However, the absorbance and emission spectra for EvaGreen, HNB, and their combination in 8 mM magnesium, the concentration of the magnesium in the LAMP reaction solution, and the corresponding spectra in the LAMP reaction mixture have key differences. The absorbance spectra in the LAMP reaction is shifted towards higher wavelengths when compared to the magnesium buffered solution. Additionally, the emission spectra for the EvaGreen, HNB, and dye combination have differing profiles in the LAMP reaction mixture versus the magnesium buffered solution. For example, in the condition without DNA in 8mM magnesium, EvaGreen has two peaks near 535

and 640 nm, whereas for EvaGreen in the LAMP reaction, there is a single markedly higher peak near 535 nm. These differences suggest that the shift in absorbance spectra from the addition of magnesium is not the sole reason for the decrease in emission at 535 nm for the dye combination in the absence of DNA. Of particular note is the difference in fluorescence spectra of the dye combination before and after amplification using LAMP. The baseline fluorescence emission at 535 nm is reduced by the addition of HNB to the solution with EvaGreen, and the emission after amplification occurs, 60 minutes later, can be easily distinguished from pre-amplification.

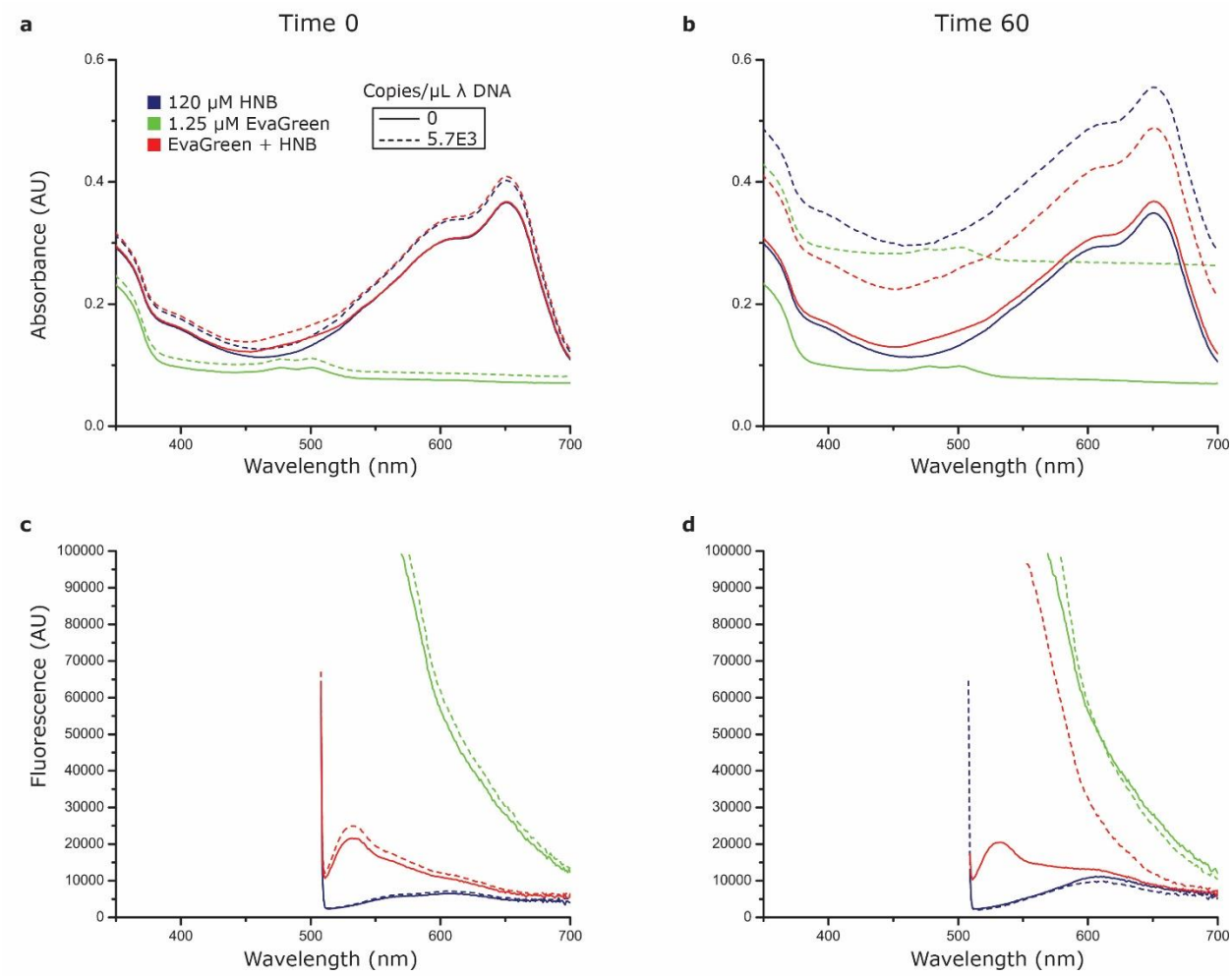

Figure 3.4 *Absorbance spectra for 1.25 μM EvaGreen and 120 μM HNB a. before (time 0) and b. after 60 minutes of LAMP amplification; emission spectra for 1.25 μM EvaGreen and 120 μM HNB c. before (time 0) and d. after 60 minutes of LAMP amplification*

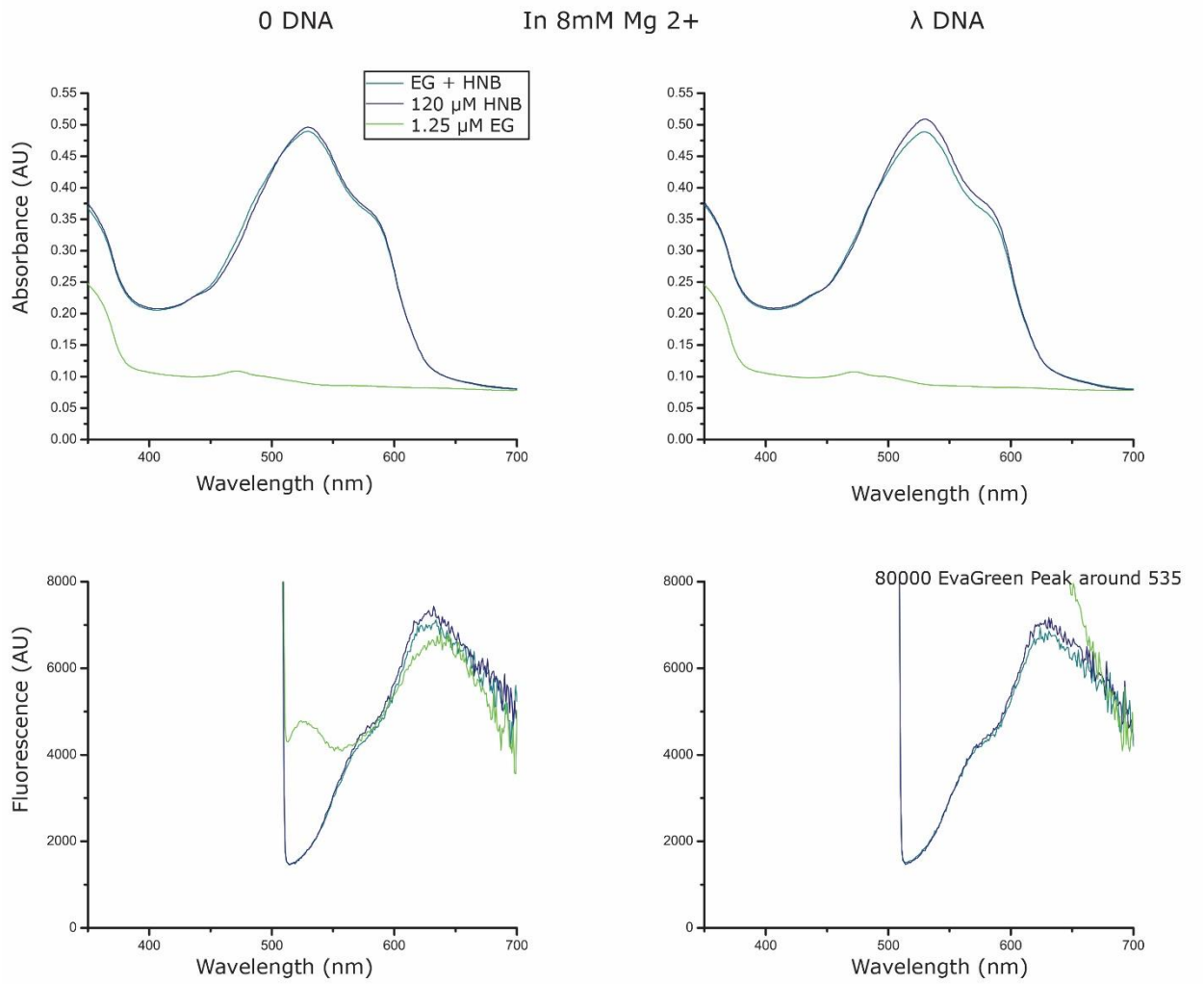

Figure 3.5 *Absorbance and emission spectra for 1.25 μM EvaGreen and 120 μM HNB in 8 mM magnesium with and without λ DNA.*

The emission spectra for acridine orange is very similar in profile to EvaGreen, with a single peak near 535 nm. As EvaGreen is a dimer of acridine orange, it follows that the emission spectra would be related. Like EvaGreen, the emission at 535 nm is diminished by the addition of HNB to a solution containing acridine orange, and the significant increase in emission at 535 nm is able to be discerned when in the presence of DNA.

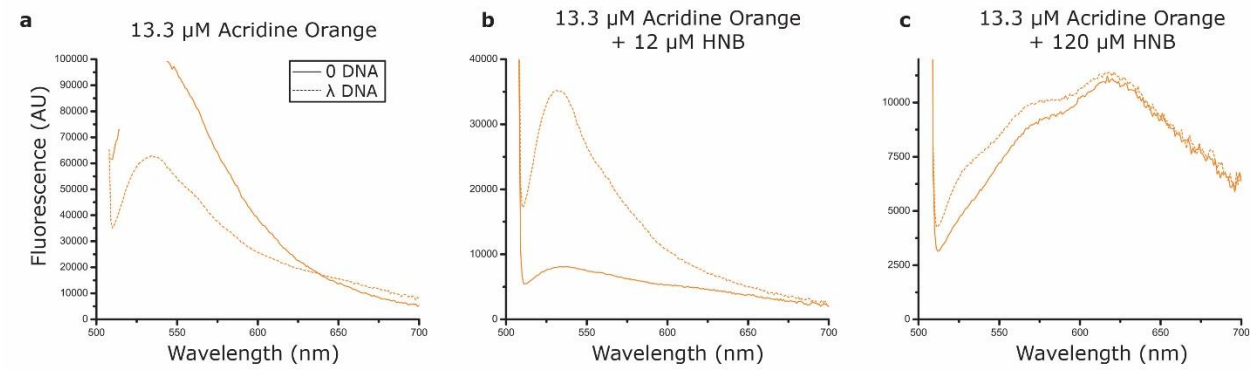

Figure 3.6 *Emission spectra for a. 13.3 µM acridine orange b. 13.3 µM acridine orange with 12 µM and c. 13.3 µM acridine orange with 120 µM HNB with and without λ DNA*

The emission spectra for SYBR Green is markedly different from both EvaGreen and acridine orange in the absence of DNA. There is a stark contrast in the emission of SYBR Green at 535 nm with and without DNA. This shows that SYBR Green is an excellent choice for intercalating dyes, as the emission is low in the absence of DNA and high in the presence of DNA. However, as shown previously in chapter two, the addition of SYBR Green prior to the start of the amplification process hinders the amount of DNA amplified such that the maximal fluorescence fold change from time 0 is still smaller than observed in solutions with both EvaGreen and HNB. Both these observations, decreased amplification in the presence of SYBR Green and the large difference in emission at 535 nm with and without DNA, suggest that the binding affinity of SYBR Green to DNA is much higher than that of EvaGreen or acridine orange. This is most likely why there does not appear to be a FRET interaction between SYBR Green and HNB in solution at these concentrations.

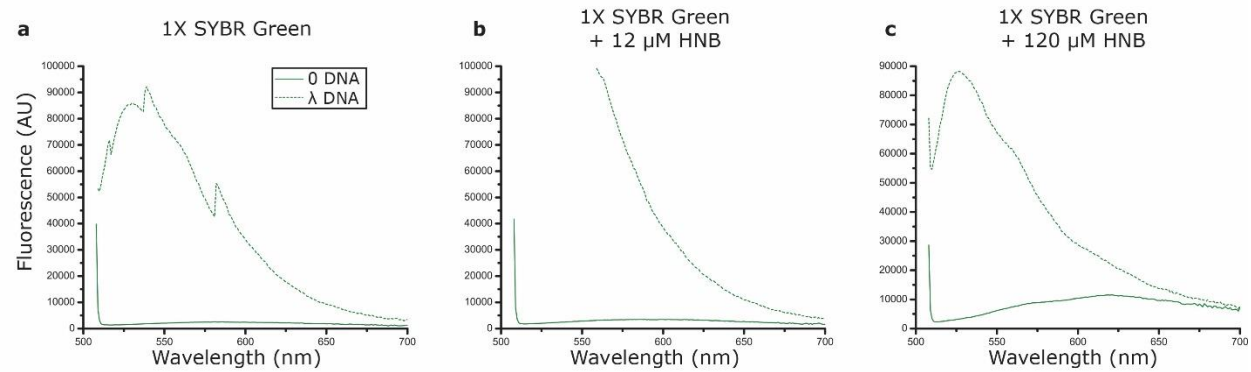

Figure 3.7 *Absorbance and emission spectra for 1X SYBR Green with 12 µM and 120 µM HNB with and without λ DNA*

Lastly, high concentrations of caffeine added to EvaGreen demonstrated similar effects as the addition of HNB to EvaGreen. The addition of caffeine generated a more stable background fluorescence, visible in the 0 polymerase negative control with increased temperature for the length of the amplification reaction. Additionally, the fluorescence fold change increased from around 2.5 to 14 with the addition of 50 mM caffeine. The absorbance spectra for caffeine shows that there is minimal absorbance across all wavelengths. This finding suggests that the improvements to the fold change and fluorescence stability with increased temperatures by the addition of caffeine to EvaGreen are not due to FRET interactions. Furthermore, the improvements in fold change between EvaGreen and HNB are a result of a combination of FRET effects and binding/sequestering interactions that mitigate interference of intercalating dyes on amplification.

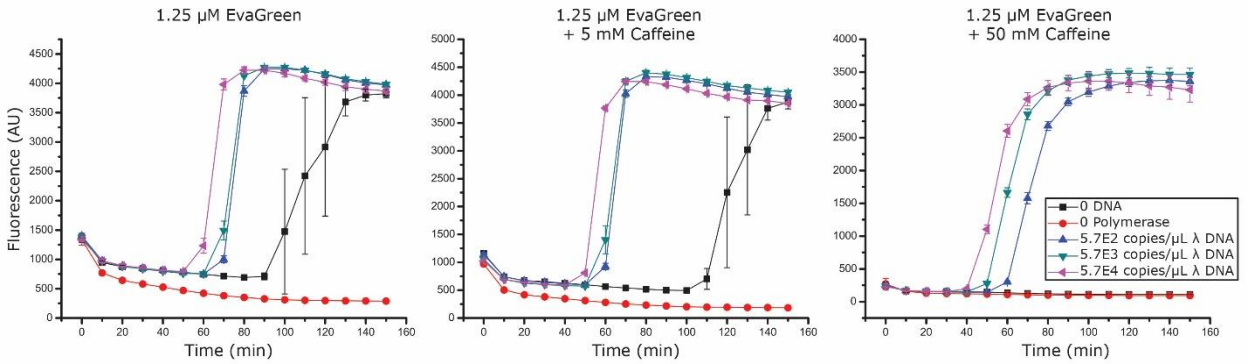

Figure 3.8. *Real-time fluorescence measurements of λ DNA amplification with loop-mediated DNA amplification (LAMP) with a. 1.25 µM EvaGreen b. 1.25 µM EvaGreen and 5 mM caffeine c. 1.25 µM EvaGreen and 50 mM caffeine. All error bars indicate s.d.*

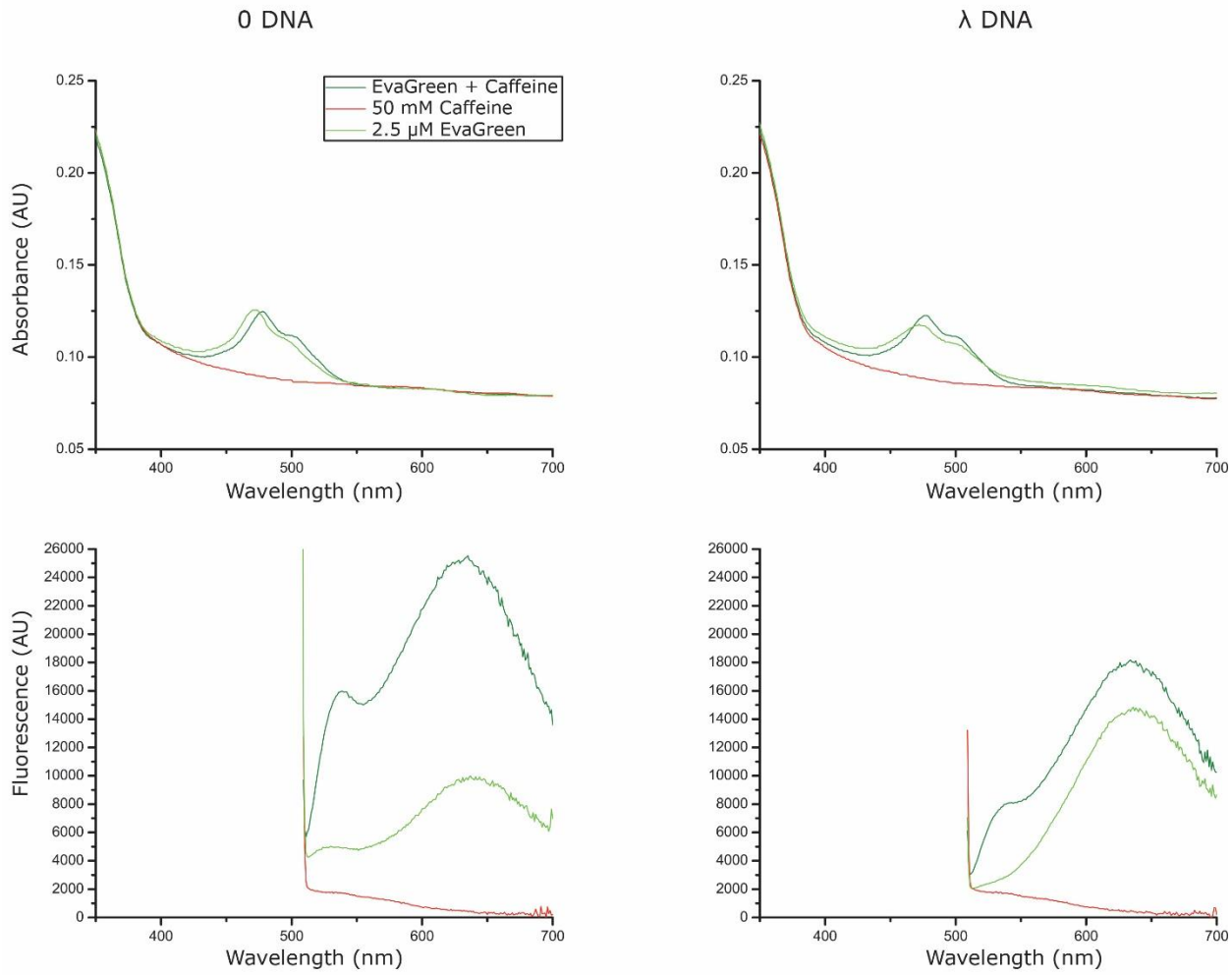

Figure 3.9. *Absorbance and emission spectra for EvaGreen and caffeine with and without λ DNA*

3.3 Conclusions

We evaluated the absorbance and emission spectra of a number of various intercalating dyes and how they were affected by the addition of various chemicals such as caffeine and HNB, both in the presence and absence of DNA. By examining the differences in absorbance spectra for caffeine and HNB, we were able to establish that the interactions between EvaGreen and caffeine or HNB are in part a result of the ability of these chemicals to sequester EvaGreen to mitigate its interference in amplification. We have also shown that FRET interactions between EvaGreen and

acridine orange occur with HNB to improve the fluorescence fold change by reducing the baseline fluorescence in solutions without DNA. These studies suggest that the two major mechanisms by which the fluorescence fold increases with the introduction of HNB are by both sequestering the intercalating dye and the subsequent FRET interactions between the dye and the chemical additive when they are in close proximity in the absence of DNA.

Further studies with other intercalating dyes such as the class of SYTO dyes should also be studied to examine the effects of the addition of HNB and caffeine. Additionally, titration studies with varying amounts of HNB in solutions of EvaGreen, acridine orange, and SYBR Green can give a deeper understanding of the binding affinities and kinetics between these dyes. Studies containing the LAMP reaction mix with and without DNA should also be examined to determine if the emission spectra are similar to the spectra for the LAMP reaction prior and post amplification. Lastly, studies with alternative amplification methods, such as qPCR, rt-PCR, or other isothermal approaches, should be conducted to determine with role of different buffers and reaction conditions.

Spectral properties for these solutions provide insight into how the intercalating dyes are interacting with additives such as caffeine and HNB. The differences in the absorbance and emission of these dyes suggest that two mechanisms in which these interactions are able to improve the fluorescence fold change above background. By understanding these mechanisms, we can now move forward to both apply these concepts to new dye combinations and also improve upon the dye combinations already investigated.

3.4 Materials and Methods

All materials were obtained from Sigma and all reactions were conducted in ultrapure DNAse and RNAse free DI water (Invitrogen) unless otherwise stated. Emission and absorbance

spectra measurements were taken at room temperature on a Biotek Cytation 5 plate reader. The LAMP reaction was performed as described previously in chapter 2. For the LAMP assay measurements, readings were taking at time 0 and after 60 minutes incubation at 65 °C for reactions without DNA, without DNA and polymerase, and with 5.7E3 copies/μL λ DNA. Absorbance and emission readings were taken for samples with and without the presence of λ DNA for various concentrations of EvaGreen, HNB, EvaGreen with HNB, acridine orange, acridine orange with HNB, SYBR Green (Thermo), SYBR Green with HNB, caffeine, and EvaGreen with caffeine.

Chapter 4: Digital Loop-mediated Isothermal DNA Amplification (LAMP)

Digital nucleic acid amplification assays are often plagued with very low signal to noise, and signal differentiation from background is often only achieved by the introduction of another dye, such as ROX, in order to determine a baseline intensity and account for any shifts in fluorescence. Digital nucleic acid amplification assays are ideal because of their unique ability to probe very small quantities of target nucleic acid in a robust and repeatable manner. Utilizing the dye combination described previously in chapter 2, digital loop-mediated isothermal DNA amplification is performed on microfluidic devices to develop a more efficient assay with a larger signal to noise than currently reported dyes. We also were able to achieve repeatable results on independent runs on separate days, demonstrating how robust the assay is. By developing the digital counterpart to the LAMP assay, we were able to further decrease the limit of detection of the assay when testing for λ DNA as the proof-of-concept target molecule.

4.1 Introduction

Nucleic acid amplification is an extremely useful tool for anything ranging from diagnostics and sequencing to genetic fingerprinting and analysis. Digital nucleic acid amplification assays are able to quantitate a small amount of target nucleic acid accurately and repeatedly without the need to generate a standard curve each time. Because digital assays operate under the principle that every compartment can be treated as a binary response to the question of whether or not the volume contains the target nucleic acid, counting of "on" versus "off" wells correlates to the amount of target nucleic acid present in the original volume. Commercialized platforms such as Fluidigm's Biomark, Raindance, or Biorad's Q200x have been used to reliably detect and quantify small amount of nucleic acid, but these systems are large and bulky, limiting

their usage to laboratory based settings. Additionally, they require separate components and/or equipment for each step of the digital PCR process: sample fractionation, thermocycling, and imaging. Several other digital platforms have been successfully developed[8,24] to detect and quantify nucleic acid. Isothermal amplification techniques are well suited for digital assays because a single temperature requirement decreases the assay complexity, simplifying the process. Even still, with isothermal amplification techniques, assay efficiency is still limited. While there are some inefficiencies inherent in the use of polymerase or perhaps due to non-specific binding interactions, some inefficiencies are present as a result of decreased amplification when intercalating dyes are present in the reaction solution. Alternatively, the fluorescent signal generated may not be large enough to be distinguished from the background. Typically, digital nucleic acid amplification assays have a very low signal to noise, often ranging from 2 to 6.5[24], even after the baseline drift is established and removed.

4.2 Results and Discussion

As has been demonstrated previously, the addition of hydroxynapthol blue (HNB) to a LAMP reaction containing the intercalating dye, EvaGreen, acts to reduce the initial background fluorescence as well as mitigate the interference that intercalating dyes have on nucleic acid amplification as seen in **figure 4.1**, the addition of HNB to the reaction also improves the digital format of this assay. For the same concentration of initial λ DNA, devices containing HNB in the reaction have more "on" wells (above the set threshold), and display a larger difference in signal between "on" and "off" wells. According to poisson statistics, at this DNA concentration and well size, approximately 93% of wells should contain a minimum of one copy of λ DNA. The actual percentage of "on" wells after one hour is less than the theoretical value, suggesting that there are assay inefficiencies, possibly stemming from pipetting errors, DNA degradation, surface fouling

effects, among others. Inefficiencies in digital LAMP are not new[72] and further optimizations in the primer design, including the number of primers, choice of polymerase, assay operating conditions, dNTP concentration, etc. can be done to improve assay efficiency. However, a number of digital assays are unable to generate a high enough signal to distinguish above the background, and this is where the novelty of the unique dye combination of EvaGreen and HNB is evident.

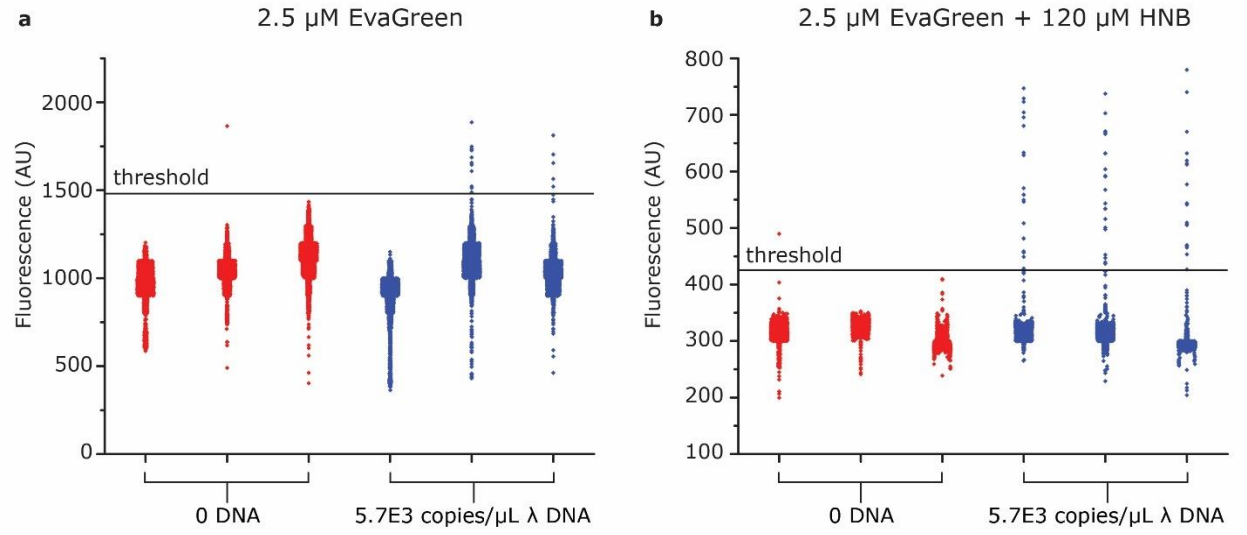

Figure 4.1 *Averaged fluorescence intensities of wells within a compression device for a negative and positive sample with λ DNA for digital LAMP with a. 2.5 µM EvaGreen and b. 2.5 µM EvaGreen and 120 µM HNB. Threshold is defined as average fluorescence intensity of 0 DNA plus ten standard deviations*

With the fluorescent signal improvements made using this unique dye combination, limit of detection (LoD) studies were then examined. As seen in **figure 4.2a**, the LoD was found to be 5.7 copies/µL. Characteristic well images are shown in **figure 4.2b**, and even at the concentration where "on" wells may not be visible to the naked eye, the intensities found from the processed images showed that wells significantly higher than background could be found in concentrations as low as 5.7 copies/µL.

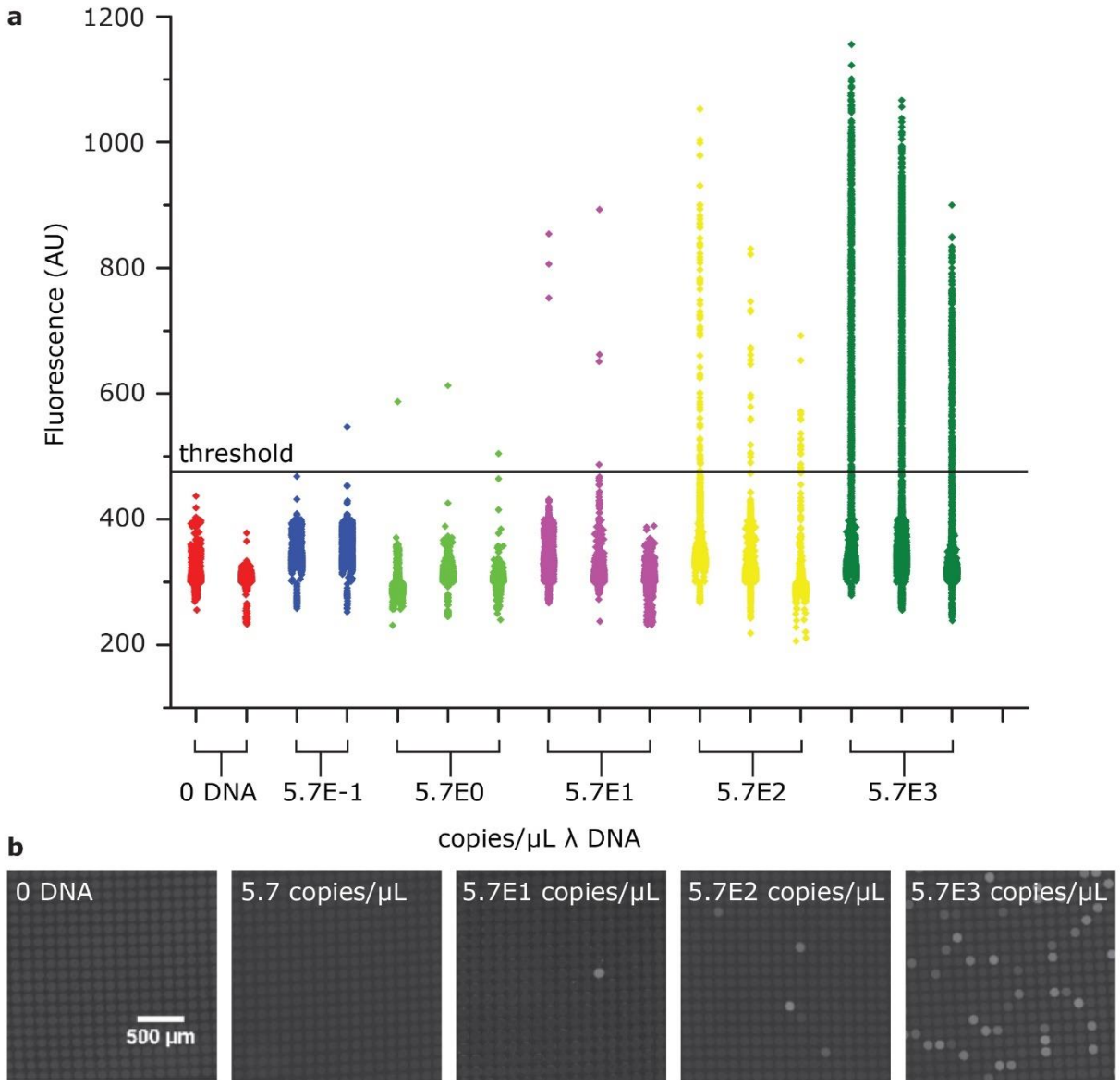

Figure 4.2 *a. Averaged fluorescence intensities of wells within a compression device for a negative sample and serial dilutions λ DNA for digital LAMP with 2.5 µM EvaGreen and 120 µM HNB. Threshold is defined as average fluorescence intensity of 0 DNA plus ten standard deviations b. Characteristic fluorescent well images of a section of the microfluidic compression device*

Lastly, assay repeatability studies were done on different days, operating under the same conditions. As shown in **figure 4.3**, the digital assay provides repeatable results across each device, spanning several days.

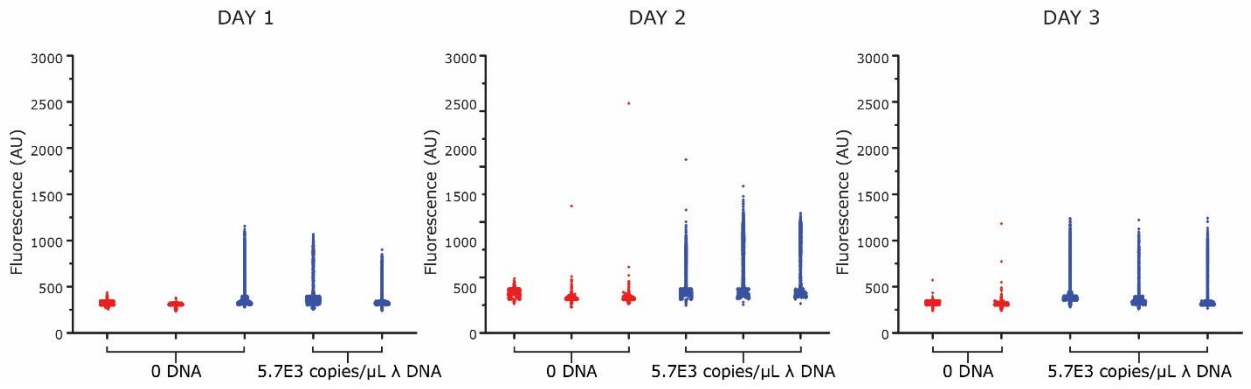

Figure 4.3 *Averaged fluorescence intensities of wells within a compression device for a negative sample and 5.7E3 copies/µL λ DNA for digital LAMP with 2.5 µM EvaGreen and 120 µM HNB.*

4.3 Conclusions

We were able to effectively demonstrate a digital assay in a two-layer PDMS compression device using LAMP for isothermal DNA amplification with a lower limit of detection than the analog version of the assay. The compression device made using standard photolithography techniques can be used to fractionate a sample into monodisperse compartments without the need for a syringe pump or an external power source. While we utilized the digitization platform to evaluate a LAMP assay, this platform can be used to easily generate monodisperse volumes, making this technology broadly applicable to more than just nucleic acid amplification techniques.

4.4 Materials and Methods

4.4.1 Compression Device Fabrication

Silicon wafer molds were fabricated using standard photolithography methods for a two-layer device (**figure 3.3a and b**). The bottom layer with a height of 5 µm was made using KMPR 1005 (MicroChem), and the top layer containing the wells with height of 60 µm was made using KMPR 1050 (MicroChem). Operating at a 10:1 ratio of base to crosslinker polydimethylsiloxane (PDMS), devices were fabricated on the silicon wafer mold, and then cut, punched, and bonded

with air plasma onto glass slides. Prior to use, the devices were placed under vacuum for one hour to facilitate device filling. The two layers allowed for the final devices to be easily filled, and due to the viscoelastic nature of PDMS, the 5 μm high first layer collapses under pressure to effectively seal off individual wells from each other.

4.4.2 Digital LAMP

The LAMP reaction was performed using the same composition as described earlier in chapter 2, with a few key changes. The polymerase concentration was doubled, and the EvaGreen concentration used was 2.5 μM. In the experiment comparing dyes, HNB was omitted from the reaction mixture with EvaGreen alone. LoD studies were performed by adding serially diluted λ DNA. The complete reaction solution was then added to the devices described previously and then the device is placed in a compression holder and the compression piece is lowered to mechanically compress and confine the reaction solution to individual wells. Each reaction is replicated in three devices, and once all devices in a single run have been filled and compressed, the devices and their holders are placed in a 67°C oven on top of a large aluminum sheet (McMaster-Carr) in order to maintain temperature stability for one hour. Afterwards, the devices are removed from the oven, and allowed to cool to room temperature before imaging. All of the devices were imaged on a Nikon Ti fluorescence microscope using large scan stitched imaging with an ASI automated stage attachment. Micrographs are then automatically analyzed in Python, as detailed below.

4.4.3 Image Processing and Normalization

Images are processed in Python so that the average normalized intensity of each individual well is calculated, and then each well is plotted as an individual data point. An intensity threshold is applied to the contrast adjusted image to determine the well locations, which are then used to

map the locations of the well centers onto the original image. The number of detected wells is validated against the predicted number of wells, calculated from the image dimensions, to ensure accuracy. If not, the threshold for the image is adjusted accordingly. Once the well centers have been located, a 100x100 pixel square around the center of each well is taken, and the resulting 10,000 pixels are used to determine the average well intensity. Next, normalization for each well is performed by calculating the average background intensity surrounding each well. The intensities outside the well are obtained from a 198x198 pixel square centered around the well, while the intensities inside the well are excluded through a 95-pixel radius circular mask. Averaging the resulting intensities gives the average background intensity for each well.

Chapter 5: Conclusions

Digital assays have shown great promise in the field of diagnostics, improving assay repeatability, lowering the assay limit of detection, and moving closer to absolute quantification by counting wells or droplets. While able to improve upon these aspects of nucleic acid amplification assays, digitization typically requires complex equipment and lengthy protocols, making the assays limited to laboratory based settings. In this work, various aspects of a digital point-of-care assay were developed, including: an improved signal generation technique, a device for digitization, and integration with mobile phone based readouts. While each of these tools and techniques developed can be used to improve various aspects of a single point-of-care assay, they are also broadly applicable to a number of other assays and techniques. For example, the unique dye combination could be useful for a number of nucleic acid amplification techniques, including qPCR, rt-PCR, and alternative isothermal amplification methods. The addition of the dye prior to the start of the assay allows for the simplification of the assay, enabling the use of this nucleic acid amplification technique with assays where multi-step additions or wash steps are not possible and may be limited by a low fluorescent signal to noise.

This nucleic acid amplification method can be used in a digital droplet format, employing various droplet generation techniques[4,73]. The use of droplets versus wells can be advantageous because of the lack of surface effects on the amplification reaction. The integration of the unique dye combination can be used to combat low signal generation issues that typically occur in digital systems. The improved signal can allow for low-cost, mobile detection systems to be used for optical detection of nucleic acid assays where a benchtop system may typically have been required.

This assay can also be integrated into immunoassays, where the signal generated from a sandwich assay is provided by the amplification of a piece of conjugated nucleotide. In preliminary

studies we have shown that LAMP products (dumbbells or longer strands) amplify more readily than linear DNA, making them ideal targets for the conjugated DNA strand. We have also proposed that by conjugating the other antibody of the sandwich pair with a polymerase, one can make a fully homogeneous digital immunoassay. In a digital assay construct, when both conjugated antibodies are present in low concentrations, the presence of the target analyte forms a sandwich complex that brings together both conjugated antibodies in a well or droplet. Once the sample is heated, isothermal amplification takes place for compartments containing both the DNA and polymerase, creating a positive signal for wells containing the target analyte.

Like other nucleic acid amplification techniques, this assay can be modified to test for specific target DNA or RNA. For example, one can perform single-cell genomic studies for cells encapsulated in droplets containing reaction mix. Additionally, further studies should be done to ensure the assay efficacy with various sample matrices. Preliminary studies showed that the LAMP assay worked with the addition of 10% cell lysate and blood plasma, but that the addition of this amount of whole blood may hinder the amplification process.

Lastly, further optimizations to improve nucleic acid amplification can be studied. Some changes to the protocol that can be made, but are not limited to, include, varying the amount of magnesium, dNTPs, polymerase, and primers in the reaction mix. It has also been shown that the optimal primers for analog nucleic acid amplification reactions may not be directly translatable as the optimal primers for a digital assay[72]. This may also be true for the concentrations of reactants as well, so further studies should be conducted to ensure the digital assay is operating at optimal conditions as well.

Appendix A

Supporting information for Chapter 2

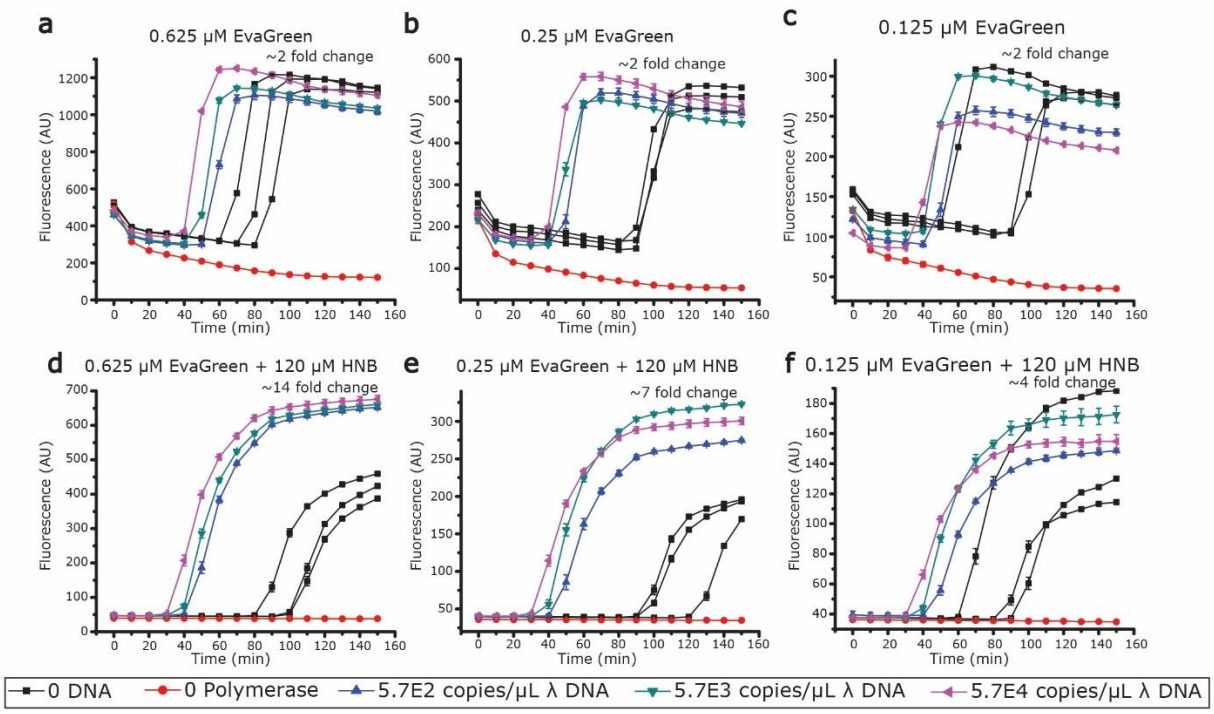

Figure 1. Real-time fluorescence measurements of λ DNA amplification with loop-mediated DNA amplification (LAMP) with a. 0.625 µM EvaGreen b. 0.25 µM EvaGreen c. 0.125 µM EvaGreen, as well as d. 0.625 µM EvaGreen and 120 µM HNB e. 0.25 µM EvaGreen and 120 µM HNB, and f. 0.125 µM EvaGreen and 120 µM HNB. Each replicate of the 0 DNA condition is shown separately as this condition is prone to contamination.

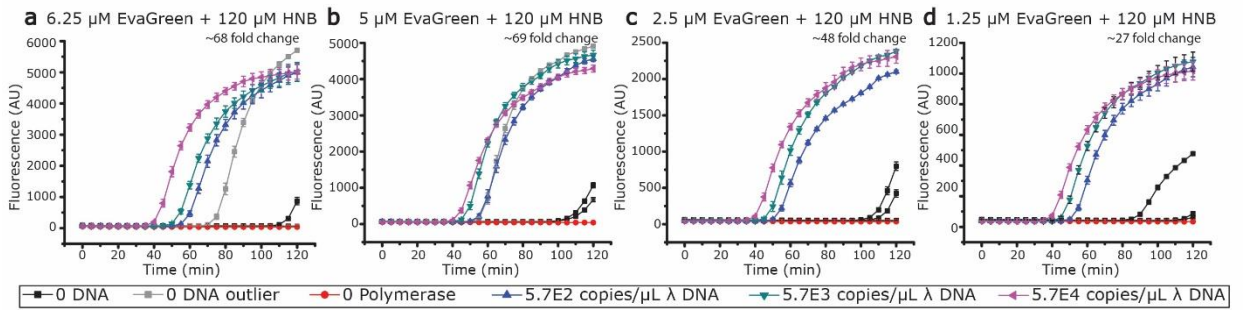

Figure 2. Real-time fluorescence measurements of λ DNA amplification with loop-mediated DNA amplification (LAMP) using 120 µM HNB and a. 6.25 µM EvaGreen b. 5 µM EvaGreen c. 2.5 µM EvaGreen and d. 1.25 µM EvaGreen

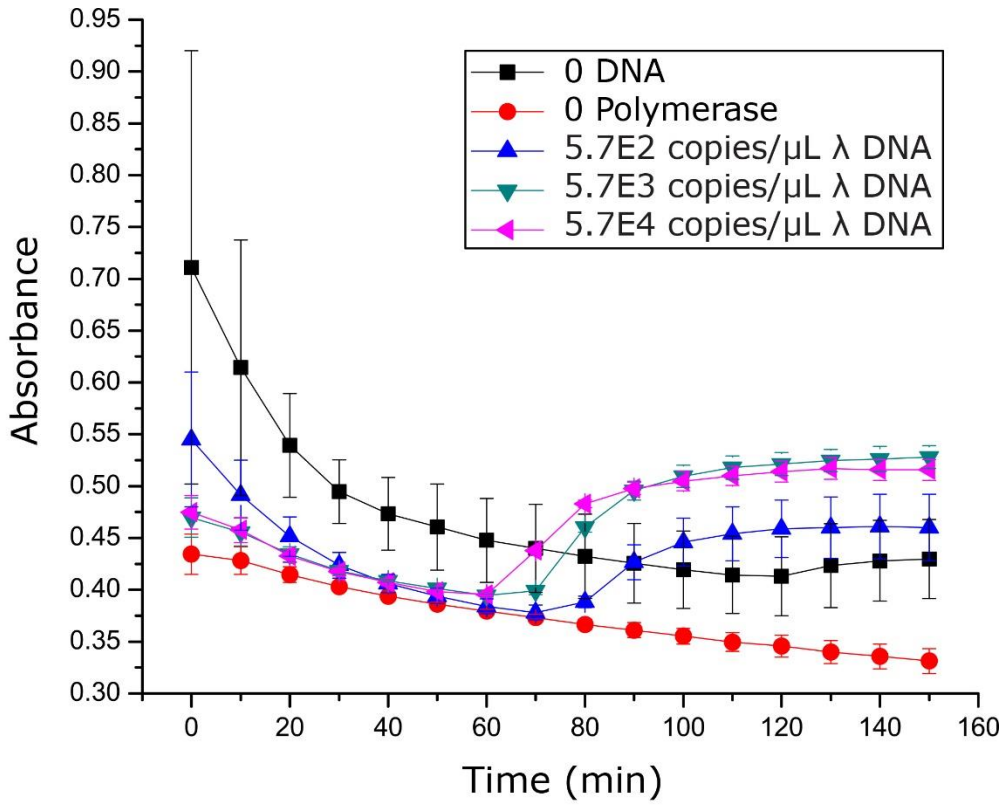

Figure 3. Real-time absorbance measurements at 650 nm of λ DNA amplification with loop-mediated DNA amplification (LAMP) using 120 µM HNB

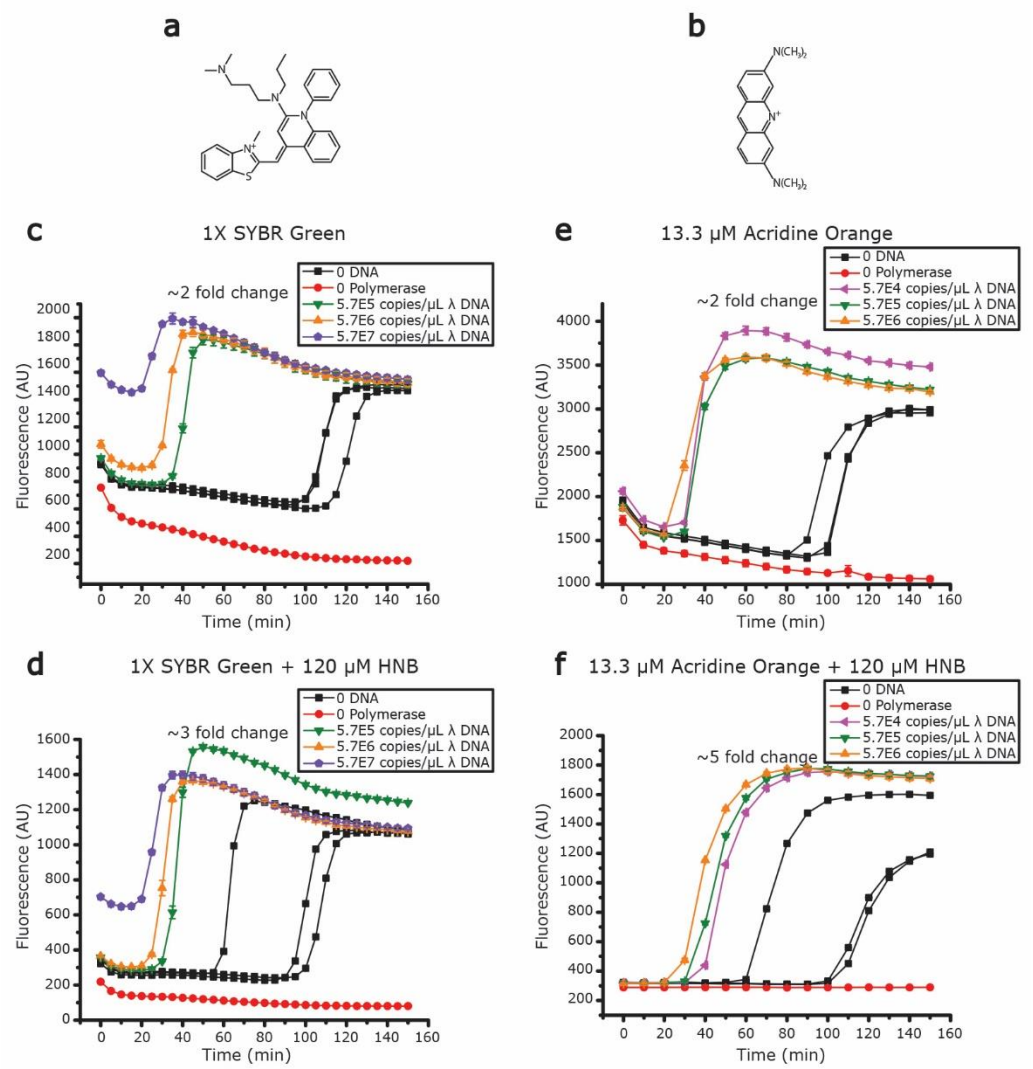

Figure 4. Chemical structures of a. SYBR Green and b. Acridine Orange; Real-time fluorescence measurements of λ DNA amplification with loop-mediated DNA amplification (LAMP) with c. 1X SYBR Green. d. 1X SYBR Green and 120 µM HNB e. 13.3 µM Acridine Orange, and f. 13.3 µM Acridine Orange and 120 µM HNB. Each replicate of the 0 DNA condition is shown separately as this condition is prone to contamination.

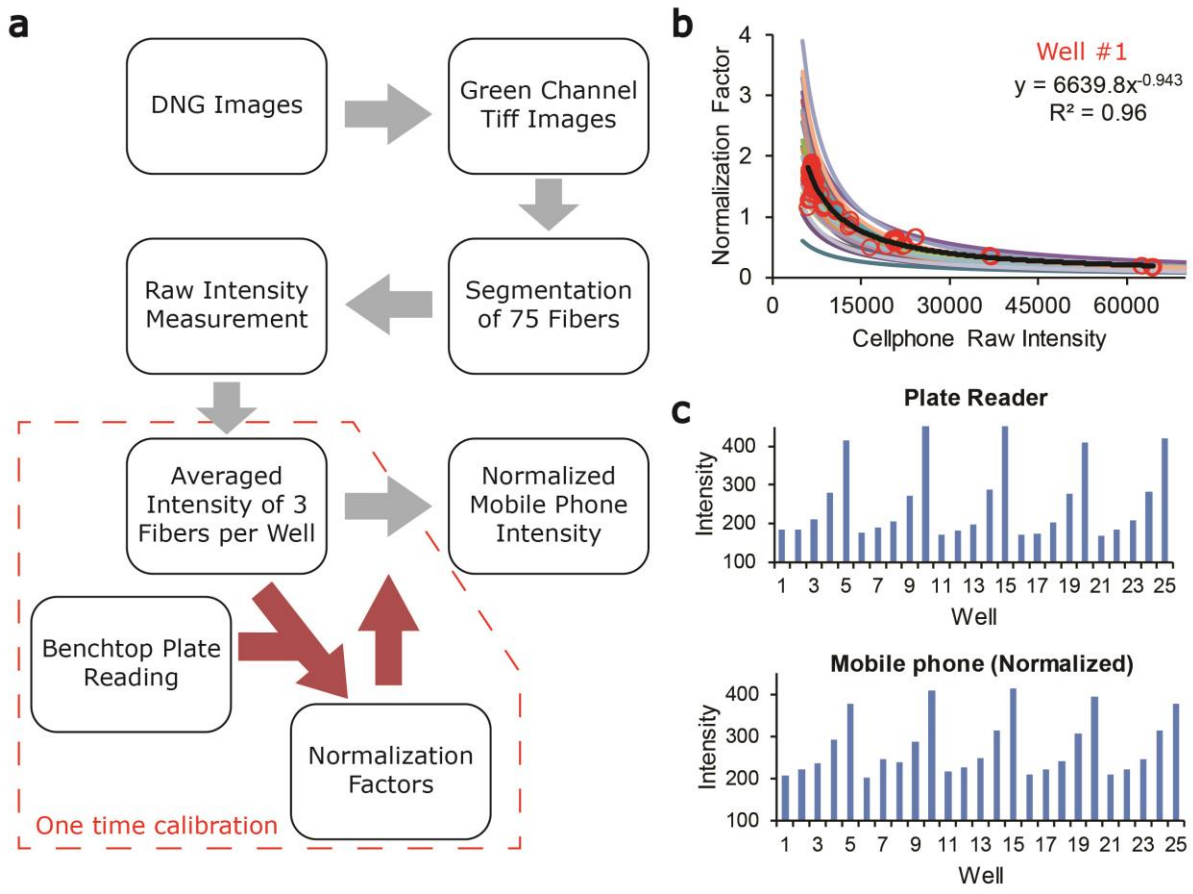

Figure 5. Scheme of image processing and device calibration. (a) Flow chart of the mobile phone image processing steps. (b) Calibration functions for all 25 wells with Well #1 highlighted in bold black curve together with its original data points in red circles. (c) A comparison of fluorescence readings between the conventional benchtop plate reader and the mobile phone reader device for fluorescein solutions.

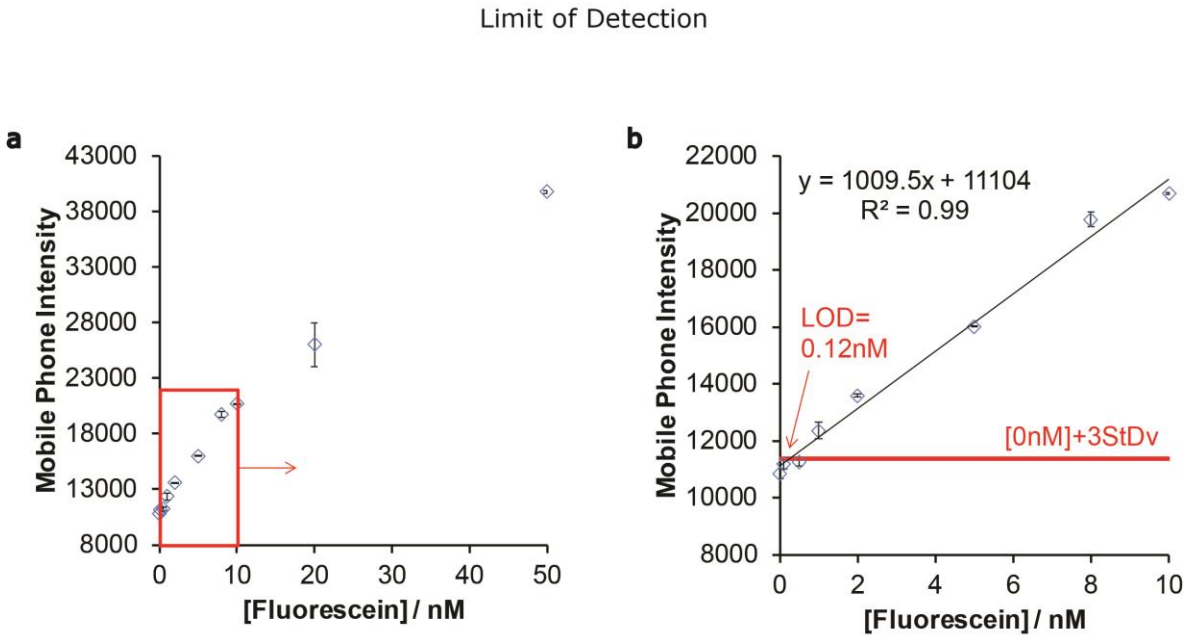

Figure 6. Limit of detection of the mobile phone fluorescence reader device. (a) Cellphone intensity versus fluorescein concentration titration curve from well #1 position. (b) Zoomed-in region from (a), showing a good linear regression and threshold (solid red line) based on 3 times of standard deviation of the blank to determine the LODs.

Table 1. Limit of Detection

Well	LODs / nM
1	0.12
2	0.13
3	0.60
4	0.14
5	0.09
6	0.10
7	0.50
8	0.33
9	0.19
10	0.10
11	0.10
12	0.20
13	0.08
14	0.33
15	0.11
16	0.10
17	0.03
18	0.21
19	0.10
20	0.06
21	0.37
22	0.09
23	0.18
24	0.07
25	0.10
Average LOD	0.18

Table 1. A list of LODs of all 25 wells of the mobile reader device for detection of fluorescein.

References

(1) Whitesides, G. M. The Origins and the Future of Microfluidics. *Nature* **2006**, *442*, 368–373.

(2) Kim, D.; Wei, Q.; Kong, J. E.; Ozcan, A.; Di Carlo, D. Research Highlights: Digital Assays on Chip. *Lab Chip* **2015**, *15*, 17–22.

(3) Rissin, D. M.; Kan, C. W.; Campbell, T. G.; Howes, S. C.; Fournier, D. R.; Song, L.; Piech, T.; Patel, P. P.; Chang, L.; Rivnak, A. J.; *et al.* Single-Molecule Enzyme-Linked Immunosorbent Assay Detects Serum Proteins at Subfemtomolar Concentrations. *Nat. Biotechnol.* **2010**, *28*, 595–599.

(4) Aigrain, L.; Gu, Y.; Quail, M. A. Quantitation of next Generation Sequencing Library Preparation Protocol Efficiencies Using Droplet Digital PCR Assays - a Systematic Comparison of DNA Library Preparation Kits for Illumina Sequencing. *BMC Genomics* **2016**, *17*, 458.

(5) Hindson, B. J.; Ness, K. D.; Masquelier, D. A.; Belgrader, P.; Heredia, N. J.; Makarewicz, A. J.; Bright, I. J.; Lucero, M. Y.; Hiddessen, A. L.; Legler, T. C.; *et al.* High-Throughput Droplet Digital PCR System for Absolute Quantitation of DNA Copy Number. *Anal. Chem.* **2011**, *83*, 8604–8610.

(6) Ottesen, E. A.; Hong, J. W.; Quake, S. R.; Leadbetter, J. R. Environmental Bacteria. *Science (80-.).* **2006**, 1464–1467.

(7) Shen, F.; Sun, B.; Kreutz, J. E.; Davydova, E. K.; Du, W.; Reddy, P. L.; Joseph, L. J.; Ismagilov, R. F. Multiplexed Quantification of Nucleic Acids with Large Dynamic Range Using Multivolume Digital RT-PCR on a Rotational SlipChip Tested with HIV and Hepatitis C Viral Load. *J. Am. Chem. Soc.* **2011**, *133*, 17705–17712.

(8) Sun, B.; Shen, F.; McCalla, S. E.; Kreutz, J. E.; Karymov, M. A.; Ismagilov, R. F. Mechanistic Evaluation of the Pros and Cons of Digital RT-LAMP for HIV-1 Viral Load Quantification on a Microfluidic Device and Improved Efficiency via a Two-Step Digital Protocol. *Anal. Chem.* **2013**, *85*, 1540–1546.

(9) Shen, F.; Du, W.; Kreutz, J. E.; Fok, A.; Ismagilov, R. F. Digital PCR on a SlipChip. *Lab Chip* **2010**, *10*, 2666.

(10) Teh, S.-Y.; Lin, R.; Hung, L.-H.; Lee, A. P. Droplet Microfluidics. *Lab Chip* **2008**, *8*, 198–220.

(11) Link, D. R.; Grasland-Mongrain, E.; Duri, A.; Sarrazin, F.; Cheng, Z.; Cristobal, G.; Marquez, M.; Weitz, D. A. Electric Control of Droplets in Microfluidic Devices. *Angew. Chemie - Int. Ed.* **2006**, *45*, 2556–2560.

(12) Niu, X.; Gulati, S.; Edel, J. B.; deMello, A. J. Pillar-Induced Droplet Merging in Microfluidic Circuits. *Lab Chip* **2008**, *8*, 1837–1841.

(13) Um, E.; Lee, D. S.; Pyo, H. B.; Park, J. K. Continuous Generation of Hydrogel Beads and Encapsulation of Biological Materials Using a Microfluidic Droplet-Merging Channel. *Microfluid. Nanofluidics* **2008**, *5*, 541–549.

(14) Yobas, L.; Martens, S.; Ong, W.-L.; Ranganathan, N. High-Performance Flow-Focusing Geometry for Spontaneous Generation of Monodispersed Droplets. *Lab Chip* **2006**, *6*, 1073–1079.

(15) Baker, M. Digital PCR Hits Its Stride. *Nat. Methods* **2012**, *9*, 541–544.

(16) Vogelstein, B.; Kinzler, K. W. Digital PCR. *Proc. Natl. Acad. Sci. U. S. A.* **1999**, *96*, 9236–9241.

(17) Nixon, G.; Garson, J. a; Grant, P.; Nastouli, E.; Foy, C. a; Huggett, J. F. Comparative Study of Sensitivity, Linearity, and Resistance to Inhibition of Digital and Nondigital Polymerase

Chain Reaction and Loop Mediated Isothermal Ampli Fi Cation Assays for Quanti Fi Cation of Human Cytomegalovirus. *Anal. Chem.* **2014**, *86*, 4387–4394.

(18) Sanders, R.; Huggett, J. F.; Bushell, C. A.; Cowen, S.; Scott, D. J.; Foy, C. A. Evaluation of Digital PCR for Absolute DNA Quantification. *Anal. Chem.* **2011**, *83*, 6474–6484.

(19) Huggett, J. F.; Whale, A. Digital PCR as a Novel Technology and Its Potential Implications for Molecular Diagnostics. *Clin. Chem.* **2013**, *59*, 1691–1693.

(20) Notomi, T.; Okayama, H. Loop-Mediated Isothermal Amplification of DNA. *Nucleic Acids Res.* **2000**, *28*, e63.

(21) Walker, G. T.; Fraiser, M. S.; Schram, J. L.; Little, M. C.; Nadeau, J. G.; Malinowski, D. P. Strand Displacement Amplification--an Isothermal, in Vitro DNA Amplification Technique. *Nucleic Acids Res.* **1992**, *20*, 1691–1696.

(22) Lizardi, P. M.; Huang, X.; Zhu, Z.; Bray-Ward, P.; Thomas, D. C.; Ward, D. C. Mutation Detection and Single-Molecule Counting Using Isothermal Rolling-Circle Amplification. *Nat Genet* **1998**, *19*, 225–232.

(23) Walker, G. T.; Little, M. C.; Nadeau, J. G.; Shank, D. D. Isothermal in Vitro Amplification of DNA by a Restriction enzyme/DNA Polymerase System. *Proc. Natl. Acad. Sci. U. S. A.* **1992**, *89*, 392–396.

(24) Rane, T.; Chen, L.; Zec, H.; Wang, T. Microfluidic Continuous Flow Digital Loop-Mediated Isothermal Amplification (LAMP). *Lab Chip* **2014**, *15*, 776–782.

(25) Leirs, K.; Tewari Kumar, P.; Decrop, D.; P??rez-Ruiz, E.; Leblebici, P.; Van Kelst, B.; Compernolle, G.; Meeuws, H.; Van Wesenbeeck, L.; Lagatie, O.; *et al.* Bioassay Development for Ultrasensitive Detection of Influenza A Nucleoprotein Using Digital ELISA. *Anal. Chem.* **2016**, *88*, 8450–8458.

(26) Rissin, D. M.; Kan, C. W.; Song, L.; Rivnak, A. J.; Fishburn, M. W.; Shao, Q.; Piech, T.;

Ferrell, E. P.; Meyer, R. E.; Campbell, T. G.; *et al.* Multiplexed Single Molecule Immunoassays. *Lab Chip* **2013**, *13*, 2902–2911.

(27) Kim, S. H.; Iwai, S.; Araki, S.; Sakakihara, S.; Iino, R.; Noji, H. Large-Scale Femtoliter Droplet Array for Digital Counting of Single Biomolecules. *Lab Chip* **2012**, *12*, 4986–4991.

(28) Rissin, D. M.; Fournier, D. R.; Piech, T.; Kan, C. W.; Campbell, T. G.; Song, L.; Chang, L.; Rivnak, A. J.; Patel, P. P.; Provuncher, G. K.; *et al.* Simultaneous Detection of Single Molecules and Singulated Ensembles of Molecules Enables Immunoassays with Broad Dynamic Range. *Anal. Chem.* **2011**, *83*, 2279–2285.

(29) Lagus, T. P.; Edd, J. F. A Review of the Theory, Methods and Recent Applications of High-Throughput Single-Cell Droplet Microfluidics. *J. Phys. D. Appl. Phys.* **2013**, *46*, 114005.

(30) Mazutis, L.; Gilbert, J.; Ung, W. L.; Weitz, D. A.; Griffiths, A. D.; Heyman, J. A. Single-Cell Analysis and Sorting Using Droplet-Based Microfluidics. *Nat. Protoc.* **2013**, *8*, 870–891.

(31) Brouzes, E.; Medkova, M.; Savenelli, N.; Marran, D.; Twardowski, M.; Hutchison, J. B.; Rothberg, J. M.; Link, D. R.; Perrimon, N.; Samuels, M. L. Droplet Microfluidic Technology for Single-Cell High-Throughput Screening. *Proc. Natl. Acad. Sci. U. S. A.* **2009**, *106*, 14195–14200.

(32) Njiru, Z. K.; Ouma, J. O.; Bateta, R.; Njeru, S. E.; Ndungu, K.; Gitonga, P. K.; Guya, S.; Traub, R. Loop-Mediated Isothermal Amplification Test for Trypanosoma Vivax Based on Satellite Repeat DNA. *Vet. Parasitol.* **2011**, *180*, 358–362.

(33) Lanciotti, R. S.; Kerst, A. J.; Kerst, A. M. Y. J. Nucleic Acid Sequence-Based Amplification Assays for Rapid Detection of West Nile and St . Louis Encephalitis Viruses Nucleic Acid Sequence-Based Amplification Assays for Rapid Detection of West Nile and St . Louis Encephalitis Viruses. *J. Clin. Microbiol.* **2001**, *39*, 4506–4513.

(34) van Dongen, J. J. M.; van der Velden, V. H. J.; Brüggemann, M.; Orfao, A. Minimal Residual Disease (MRD) Diagnostics in Acute Lymphoblastic Leukemia (ALL): Need for Sensitive, Fast and Standardized Technologies. *Blood* **2015**, *125*, blood-2015-03-580027.

(35) Lewis, J. M.; Heineck, D. P.; Heller, M. J. Detecting Cancer Biomarkers in Blood: Challenges for New Molecular Diagnostic and Point-of-Care Tests Using Cell-Free Nucleic Acids. *Expert Rev. Mol. Diagn.* **2015**, *15*, 1187–1200.

(36) Niemz, A.; Ferguson, T. M.; Boyle, D. S. Point-of-Care Nucleic Acid Testing for Infectious Diseases. *Trends Biotechnol.* **2011**, *29*, 240–250.

(37) Dineva, M. A.; Mahilum-Tapay, L.; Lee, H. Sample Preparation: A Challenge in the Development of Point-of-Care Nucleic Acid-Based Assays for Resource-Limited Settings. *Analyst* **2007**, *132*, 1193.

(38) Marx, V. PCR Heads into the Field. *Nat. Methods* **2015**, *12*, 393–397.

(39) Ahmed, M. U.; Saaem, I.; Wu, P. C.; Brown, A. S. Personalized Diagnostics and Biosensors: A Review of the Biology and Technology Needed for Personalized Medicine. *Crit. Rev. Biotechnol.* **2014**, *34*, 180–196.

(40) Cordray, M. S.; Richards-Kortum, R. R. Review: Emerging Nucleic Acid-Based Tests for Point-of-Care Detection of Malaria. *Am. J. Trop. Med. Hyg.* **2012**, *87*, 223–230.

(41) Yan, L.; Zhou, J.; Zheng, Y.; Gamson, A. S.; Roembke, B. T.; Nakayama, S.; Sintim, H. O. Isothermal Amplified Detection of DNA and RNA. *Mol. Biosyst.* **2014**, *10*, 970–1003.

(42) Lafleur, L.; Bishop, J. D.; Heiniger, E. K.; Gallagher, R. P.; Wheeler, M. D.; Kauffman, P. C.; Zhang, X.; Kline, E.; Buser, J.; Kumar, S.; *et al.* A Rapid, Instrument-Free, Sample-to-Result Nucleic Acid Amplification Test. *Lab Chip* **2016**.

(43) Nagamine, K.; Hase, T.; Notomi, T. Accelerated Reaction by Loop-Mediated Isothermal Amplification Using Loop Primers. *Mol. Cell. Probes* **2002**, *16*, 223–229.

(44) Liao, S. C.; Peng, J.; Mauk, M. G.; Awasthi, S.; Song, J.; Friedman, H.; Bau, H. H.; Liu, C. Smart Cup: A Minimally-Instrumented, Smartphone-Based Point-of-Care Molecular Diagnostic Device. *Sensors Actuators, B Chem.* **2016**, *229*, 232–238.

(45) Son, J. H.; Cho, B.; Hong, S.; Lee, S. H.; Hoxha, O.; Haack, A. J.; Lee, L. P. Ultrafast Photonic PCR. *Light Sci. Appl.* **2015**, *4*, e280.

(46) Cox, J. O.; Decarmen, T. S.; Ouyang, Y.; Strachan, B.; Connon, C.; Gibson, K.; Jackson, K.; Landers, J. P. A Novel , Integrated Forensic Microdevice on a Rotation-Driven Platform : Buccal Swab to STR Product in Less than Two Hours. **2011**, 1–29.

(47) Parida, M.; Sannarangaiah, S.; Kumar, P.; Rao, P. V. L.; Morita, K. Loop Mediated Isothermal Amplification (LAMP): A New Generation of Innovative Gene Amplification Technique; Perspectives in Clinical Diagnosis of Infectious Diseases. *Rev. Med. Virol.* **2008**, *18*, 407–421.

(48) Ahmad, F.; Hashsham, S. A. Miniaturized Nucleic Acid Amplification Systems for Rapid and Point-of-Care Diagnostics: A Review. *Anal. Chim. Acta* **2012**, *733*, 1–15.

(49) Monis, P. T.; Giglio, S.; Saint, C. P. Comparison of SYTO9 and SYBR Green I for Real-Time Polymerase Chain Reaction and Investigation of the Effect of Dye Concentration on Amplification and DNA Melting Curve Analysis. *Anal. Biochem.* **2005**, *340*, 24–34.

(50) Mao, F.; Leung, W.-Y.; Xin, X. Characterization of EvaGreen and the Implication of Its Physicochemical Properties for qPCR Applications. *BMC Biotechnol.* **2007**, *7*, 76.

(51) Gudnason, H.; Dufva, M.; Bang, D. D.; Wolff, A. Comparison of Multiple DNA Dyes for Real-Time PCR: Effects of Dye Concentration and Sequence Composition on DNA Amplification and Melting Temperature. *Nucleic Acids Res.* **2007**, *35*, 1–8.

(52) Nath, K.; Sarosy, J. W.; Hahn, J.; Di Como, C. J. Effects of Ethidium Bromide and SYBR Green I on Different Polymerase Chain Reaction Systems. *J. Biochem. Biophys. Methods*

2000, *42*, 15–29.

(53) Goto, M.; Honda, E.; Ogura, A.; Nomoto, A.; Hanaki, K. I. Colorimetric Detection of Loop-Mediated Isothermal Amplification Reaction by Using Hydroxy Naphthol Blue. *Biotechniques* **2009**, *46*, 167–172.

(54) Wastling, S. L.; Picozzi, K.; Kakembo, A. S. L.; Welburn, S. C. LAMP for Human African Trypanosomiasis: A Comparative Study of Detection Formats. *PLoS Negl. Trop. Dis.* **2010**, *4*.

(55) Toumazou, C.; Shepherd, L. M.; Reed, S. C.; Chen, G. I.; Patel, A.; Garner, D. M.; Wang, C.-J. a; Ou, C.-P.; Amin-Desai, K.; Athanasiou, P.; *et al.* Simultaneous DNA Amplification and Detection Using a pH-Sensing Semiconductor System. *Nat. Methods* **2013**, *10*, 641–646.

(56) Guiducci, C.; Spiga, F. M. Another Transistor-Based Revolution: On-Chip qPCR. *Nat. Methods* **2013**, *10*, 617–618.

(57) Vashist, S. K.; Mudanyali, O.; Schneider, E. M.; Zengerle, R.; Ozcan, A. Cellphone-Based Devices for Bioanalytical Sciences Multiplex Platforms in Diagnostics and Bioanalytics. *Anal. Bioanal. Chem.* **2014**, *406*, 3263–3277.

(58) Ozcan, A. Mobile Phones Democratize and Cultivate next-Generation Imaging, Diagnostics and Measurement Tools. *Lab Chip* **2014**, *14*, 3187–3194.

(59) Laksanasopin, T.; Guo, T. W.; Nayak, S.; Sridhara, A. a; Xie, S.; Olowookere, O. O.; Cadinu, P.; Meng, F.; Chee, N. H.; Kim, J.; *et al.* Supplementary Information: A Smartphone Dongle for Diagnosis of Infectious Diseases at the Point of Care. *Sci. Transl. Med.* **2015**, *7*, 273re1.

(60) Berg, B.; Cortazar, B.; Tseng, D.; Ozkan, H.; Feng, S.; Wei, Q.; Chan, R. Y. L.; Burbano, J.; Farooqui, Q.; Lewinski, M.; *et al.* Cellphone-Based Hand-Held Microplate Reader for

Point-of-Care Testing of Enzyme-Linked Immunosorbent Assays. *ACS Nano* **2015**, *9*, 7857–7866.

(61) Selck, D. A.; Karymov, M. A.; Sun, B.; Ismagilov, R. F. Increased Robustness of Single-Molecule Counting with Microfluidics, Digital Isothermal Amplification, and a Mobile Phone versus Real-Time Kinetic Measurements. *Anal. Chem.* **2013**, *85*, 11129–11136.

(62) Nolan, T.; Hands, R. E.; Bustin, S. a. Quantification of mRNA Using Real-Time RT-PCR. *Nat. Protoc.* **2006**, *1*, 1559–1582.

(63) Nazarenko, I.; Lowe, B.; Darfler, M.; Ikonomi, P.; Schuster, D.; Rashtchian, A. Multiplex Quantitative PCR Using Self-Quenched Primers Labeled with a Single Fluorophore. *Nucleic Acids Res.* **2002**, *30*, e37.

(64) Khairnar, K.; Martin, D.; Lau, R.; Ralevski, F.; Pillai, D. R. Multiplex Real-Time Quantitative PCR, Microscopy and Rapid Diagnostic Immuno-Chromatographic Tests for the Detection of Plasmodium Spp: Performance, Limit of Detection Analysis and Quality Assurance. *Malar. J.* **2009**, *8*, 284.

(65) Hackett, S. J.; Guiver, M.; Marsh, J.; Sills, J. a; Thomson, a P. J.; Kaczmarski, E. B.; Hart, C. a. Meningococcal Bacterial DNA Load at Presentation Correlates with Disease Severity. *Arch. Dis. Child.* **2002**, *86*, 44–46.

(66) Craw, P.; Balachandran, W. Isothermal Nucleic Acid Amplification Technologies for Point-of-Care Diagnostics: A Critical Review. *Lab Chip* **2012**, *12*, 2469–2486.

(67) Asiello, P. J.; Baeumner, A. J. Miniaturized Isothermal Nucleic Acid Amplification, a Review. *Lab Chip* **2011**, *11*, 1420–1430.

(68) Das, A.; Spackman, E.; Senne, D.; Pedersen, J.; Suarez, D. L. Development of an Internal Positive Control for Rapid Diagnosis of Avian Influenza Virus Infections by Real-Time Reverse Transcription-PCR with Lyophilized Reagents. *J. Clin. Microbiol.* **2006**, *44*, 3065–

3073.

(69) Siegmund, V.; Adjei, O.; Racz, P.; Berberich, C.; Klutse, E.; Van Vloten, F.; Kruppa, T.; Fleischer, B.; Bretzel, G. Dry-Reagent-Based PCR as a Novel Tool for Laboratory Confirmation of Clinically Diagnosed Mycobacterium Ulcerans-Associated Disease in Areas in the Tropics Where M. Ulcerans Is Endemic. *J. Clin. Microbiol.* **2005**, *43*, 271–276.

(70) Glynou, K.; Kastanis, P.; Boukouvala, S.; Tsaoussis, V.; Ioannou, P. C.; Christopoulos, T. K.; Traeger-Synodinos, J.; Kanavakis, E. High-Throughput Microtiter Well-Based Chemiluminometric Genotyping of 15 H88 Gene Mutations in a Dry-Reagent Format. *Clin. Chem.* **2007**, *53*, 384–391.

(71) Zhang, C.; Xing, D. Miniaturized PCR Chips for Nucleic Acid Amplification and Analysis: Latest Advances and Future Trends. *Nucleic Acids Res.* **2007**, *35*, 4223–4237.

(72) Khorosheva, E. M.; Karymov, M. A.; Selck, D. A.; Ismagilov, R. F. Lack of Correlation between Reaction Speed and Analytical Sensitivity in Isothermal Amplification Reveals the Value of Digital Methods for Optimization: Validation Using Digital Real-Time RT-LAMP. *Nucleic Acids Res.* **2016**, *44*, e10.

(73) Hayden, R. T.; Gu, Z.; Sam, S. S.; Sun, Y.; Tang, L.; Pounds, S.; Caliendo, A. M. Comparative Evaluation of Three Commercial Quantitative Cytomegalovirus Standards by Use of Digital and Real-Time PCR. *J. Clin. Microbiol.* **2015**, *53*, 1500–1505.